PLOS ONE

RESEARCH ARTICLE

"Stealth dissemination" of macrophage-tumor cell fusions cultured from blood of patients with pancreatic ductal adenocarcinoma

Gary A. Clawson[1]*, Gail L. Matters[2], Ping Xin[1], Christopher McGovern[2], Eric Wafula[3], Claude dePamphilis[3], Morgan Meckley[1], Joyce Wong[4], Luke Stewart[5], Christopher D'Jamoos[5], Naomi Altman[6], Yuka Imamura Kawasawa[7], Zhen Du[1], Loren Honaas[3], Thomas Abraham[8]

1 Gittlen Cancer Research Laboratories and the Department of Pathology, Hershey Medical Center (HMC), Pennsylvania State University (PSU), Hershey, PA, United States of America, **2** Department of Biochemistry & Molecular Biology, HMC, PSU, Hershey, PA, United States of America, **3** Department of Biology, Eberly College, University Park (UP), Pennsylvania State University, University Park, PA, United States of America, **4** Department of Surgery, HMC, PSU, Hershey, PA, United States of America, **5** Applications Support, Fluidigm Corporation, South San Francisco, CA, United States of America, **6** Department of Statistics, Eberly College, UP, PSU, University Park, PA, United States of America, **7** Department of Pharmacology and Biochemistry & Molecular Biology, Institute for Personalized Medicine, HMC, PSU, Hershey, PA, United States of America, **8** Department of Neural & Behavioral Sciences and Microscopy Imaging Facility, HMC, PSU, Hershey, PA, United States of America

* gac4@psu.edu, gac4gac4@gmail.com

Check for updates

OPEN ACCESS

Citation: Clawson GA, Matters GL, Xin P, McGovern C, Wafula E, dePamphilis C, et al. (2017) "Stealth dissemination" of macrophage-tumor cell fusions cultured from blood of patients with pancreatic ductal adenocarcinoma. PLoS ONE 12 (9): e0184451. https://doi.org/10.1371/journal.pone.0184451

Editor: Surinder K. Batra, University of Nebraska Medical Center, UNITED STATES

Received: March 13, 2017

Accepted: August 24, 2017

Published: September 28, 2017

Copyright: © 2017 Clawson et al. This is an open access article distributed under the terms of the Creative Commons Attribution License, which permits unrestricted use, distribution, and reproduction in any medium, provided the original author and source are credited.

Data Availability Statement: The repository information is as follows: SRA Project accession: SRP108709 (https://www.ncbi.nlm.nih.gov/sra/?term=SRP108709) and SRA BioProject accession: PRJNA389267 (https://www.ncbi.nlm.nih.gov/bioproject/PRJNA389267).

Funding: This work was supported by grants from the NIH (UL1 TR000125, 1S10OD010756-01A1 and 1S10OD018124-01A1), the Pennsylvania State Hershey Clinical and Translational Science Institute,

Abstract

Here we describe isolation and characterization of macrophage-tumor cell fusions (MTFs) from the blood of pancreatic ductal adenocarcinoma (PDAC) patients. The MTFs were generally aneuploidy, and immunophenotypic characterizations showed that the MTFs express markers characteristic of PDAC and stem cells, as well as M2-polarized macrophages. Single cell RNASeq analyses showed that the MTFs express many transcripts implicated in cancer progression, LINE1 retrotransposons, and very high levels of several long non-coding transcripts involved in metastasis (such as MALAT1). When cultured MTFs were transplanted orthotopically into mouse pancreas, they grew as obvious well-differentiated islands of cells, but they also disseminated widely throughout multiple tissues in "stealth" fashion. They were found distributed throughout multiple organs at 4, 8, or 12 weeks after transplantation (including liver, spleen, lung), occurring as single cells or small groups of cells, without formation of obvious tumors or any apparent progression over the 4 to 12 week period. We suggest that MTFs form continually during PDAC development, and that they disseminate early in cancer progression, forming "niches" at distant sites for subsequent colonization by metastasis-initiating cells.

Introduction

Pancreatic ductal adenocarcinoma (PDAC) is one of the most prevalent cancers worldwide, and is predicted to be the 2nd leading cause of cancer deaths by 2030 [1]. PDAC is generally

the National Center for Advancing Translational Science (TL1 R000125), and gift funds from the Gittlen Cancer Research Laboratories. Funding was also provided by Fluidigm. This funder provided support in the form of salaries for authors (LS and CD'J) but did not have any additional role in the study design, data collection and analysis, decision to publish, or preparation of the manuscript. The specific roles of these authors are articulated in the "author contributions" section.

Competing interests: LS and CD'J are employed by Fluidigm. This does not alter our adherence to PLOS ONE policies on sharing data and materials. The other authors have no competing interests to disclose.

diagnosed at an advanced stage due to lack of early symptoms, precluding surgical excision, and there are no effective alternative treatments. As with most carcinomas, mortality is due to metastatic dissemination, and CTCs are observed in a high proportion of PDAC patients at all stages [2, 3]. While there are a number of models for what is termed the "metastatic cascade" [4], the nature of the CTCs which actually produce metastatic foci is not clear.

Perhaps the most widely accepted hypothesis underlying metastasis is that the primary tumor microenvironment (TME) induces an epithelial-to-mesenchymal transition (EMT) in a subset of epithelial cancer cells, that facilitates their escape into the bloodstream or lymphatics [5]. A number of studies for example have documented EMT-related changes (and loss of EpCAM expression) in CTCs [6–10]. In spite of recognized shortcomings [11, 12], CellSearch quantitation of numbers of EpCAM+ CTCs in peripheral blood has prognostic significance [13–15]. However, the picture remains incomplete: Which CTCs are the capable of initiating metastatic lesions (so called metastasis initiating cells, MICs), and how do MICs find suitable sites for growth of metastatic foci [5]? With regard to the former, a corollary idea is that the EMT-altered cancer cells at the periphery of a primary tumor facilitate liberation of cancer stem cells [5, 16, 17], which could represent the MICs. In this scenario, the overall number of CTCs would stochastically represent a much smaller subset of MICs. However, this story does not address the latter question: how MICs find suitable "niches" which allow them to establish metastases and proliferate [18].

An alternative theory for metastasis [19–22] involves fusion of macrophages with tumor cells (macrophage-tumor cell fusions, **MTF**s). With some sort of sorting, recombination, and/or reprogramming [23] of genetic material, this could produce neoplastic cells which have acquired the highly invasive phenotype of macrophages. There is considerable support for this notion from animal models, and some recent support from reports of human cancers [20], but how frequently this occurs is unknown and the basic premise seems to be at odds with the EMT/stem cell hypothesis [18].

We recently reported on MTFs cultured from blood from patients with early-stage and advanced melanomas [24]. The MTFs expressed multiple markers characteristic of M2-polarized macrophages, as well as epithelial, melanocytic and stem cell markers. When the melanoma MTFs were transplanted into mice as subcutaneous xenographs, they disseminated only to pancreas, where they formed what appeared to be benign islands of well-differentiated cells. Here we report on analogous MTFs cultured from blood of PDAC patients. These cells show expression of a similar combination of macrophage and epithelial/pancreatic/stem cell markers. Ultrastructural analyses revealed a macrophage-like morphology, with extensive autophagic vacuoles, etc. Single cell RNASeq analyses showed high levels of expression of various metastasis-related markers (particularly the MIF/CD44/CD74/CXCR4 signaling axis), as well as LINE-1 retrotransposons. In addition, the MTFs uniformly expressed very high levels of MALAT1, a long non-coding RNA transcript known to be involved in control of metastasis [25, 26], as well as additional long non-coding transcripts implicated in cancer progression. When the cultured PDAC MTFs were orthotopically transplanted into the pancreas in mice, they formed well-differentiated islands there. They did not form obvious tumors in any other distant locations. However, they were found to disseminate widely throughout multiple tissues, including liver, spleen, lung, submucosa, etc. They were found as single cells or small groups of cells and often appeared large and irregularly shaped. There was no apparent progression in number of cells in various tissues over the 4 to12 week period, although the only metastatic cells found in lung were observed at 12 weeks. The MTFs also appeared to alter their expression of some markers after dissemination.

Results

Immunophenotypic analysis of cultured MTFs

Blood samples were obtained under an approved IRB protocol from patients with PDAC (some patients had early stage resectable disease, although most had advanced disease). Samples were processed as described, and cultured in standard media for ~4–6 weeks. Cells were quite sparse at the outset of culturing (perhaps a few cells/ml). Populations of cells grew from all preparations (~ 20), and they were fixed and stained for various pairs of markers and examined using confocal microscopy, including macrophage markers, pancreatic, epithelial, and pancreatic stem cell markers. The cell populations showed uniform expression (and localization) of the various pairs of human markers (**Figs 1 and 2**).

We also examined cultured MTFs for expression of the pro-carcinogenic cytokine MIF, because of MIF' s prominent roles in M2 polarization of macrophages, the tumor microenvironment (TME), and cancer progression [27–31]. The cultured PDAC MTFs routinely stained positively for the MIF (Fig 2), with some very intriguing patterns of staining noted. Many of the individual nuclei appeared to have "tunnels" through them. These tunnels (invaginations) were lined by an intact nuclear envelope, and often contained cytoplasmic organelles including mitochondria, etc. (see below). The interior (cytoplasm) within these tunnels stained strongly for MIF, as determined using 3D confocal images (for example, see Panels A1 and B1 of Fig 2). Such tunnels had previously been observed in MTFs cultured from melanoma patient samples, as well as within melanomas in situ [24], and they are also evident in human PDACs (see below).

Given the robust immunostaining for MIF, we also examined the functionally related stem cell markers CXCR4 and CD44. CXCR4 is a non-cognate receptor for MIF [32, 33] and CD44 represents the signaling component of the MIF:CD74 receptor complex [34]. As with MIF, we observed strong expression of CXCR4 and CD44, indicative of pro-carcinogenic activities of the MIF/CD44/CD74/CXCR4 signaling pathway (Fig 2; see Discussion).

Immunophenotypic analysis of primary human PDACs

We observed analogous results in tissue specimens from primary human PDACs (**Fig 3**, Panels A-X). While there was morphologic heterogeneity in various regions of the PDACs, there was a surprisingly extensive subpopulation of cells that dually stained for various pairs of macrophage, pancreatic-epithelial, and stem cell markers (Fig 3). Invaginations (tunnels) were often evident in nuclei of the dual-staining cells (as was also apparent with DAPI-stained PDACs). With 3D confocal images, we also observed dual-staining of these cells for combinations of macrophage markers (CD204 or CD206) and pancreatic cancer markers ZG16B or S100PBP (**Fig 4**). We also conducted ploidy analysis of the apparent MTFs within PDACs in situ. We found that this population of dual-staining cells contained markedly abnormal DNA contents, with a large portion of the cells showing very irregular nuclei with aneuploid DNA content (**Fig 5**). These results are similar to those we previously described for melanoma-derived MTFs [24].

Ultrastructural features of cultured MTFs

Ultrastructural examination of the MTFs via transmission electron microscopy (TEM) showed features characteristic of macrophages (**Fig 6**). The MTFs were generally large cells, which showed exuberant pseudopods, lamellipodia, and exocytosis. Nuclei generally showed very irregular (in fact, jagged) contours, as noted previously with melanoma MTFs [24]. Nuclei of the PDAC MTFs often showed "tunnels" through them (from ultrastructural examination, the

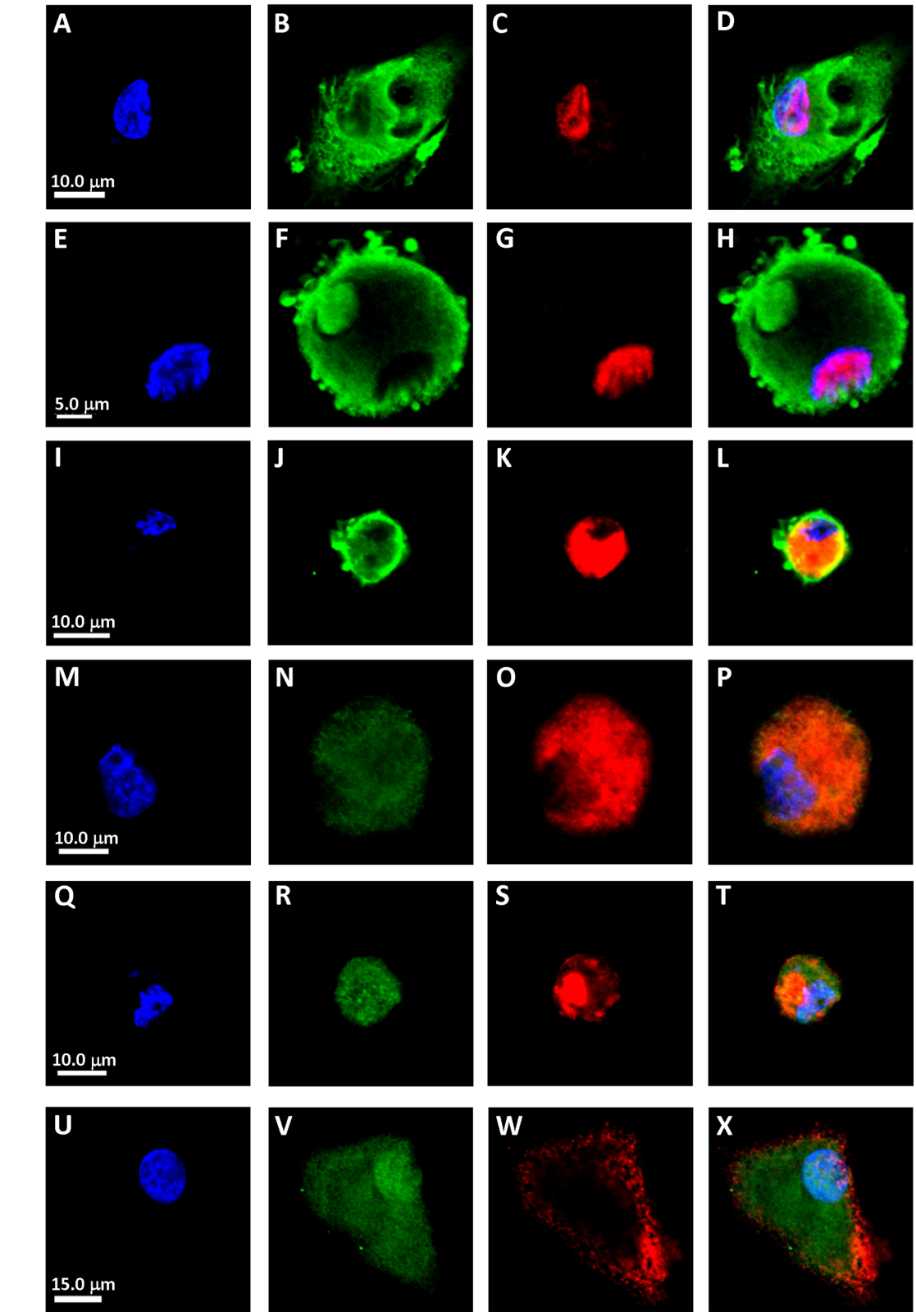
[PDAC MTFs]
A
B
C
D
10.0 μm
E
F
G
H
5.0 μm
I
J
K
L
10.0 μm
M
N
O
P
10.0 μm
Q
R
S
T
10.0 μm
U
V
W
X
15.0 μm

Fig 1. Immunostaining of cultured MTFs from PDAC patients. Representative confocal images of cultured MTFs from different PDAC patients. The cell populations showed uniform staining, and subcellular localization, of the various pairs of markers. Since the plates were sparsely populated, low power panoramic photomicrographs did not allow adequate visualization of the subcellular localizations, so photomicropraphs of individual cells were generally taken. Nuclei were stained with DAPI (Blue) shown in Panels [**A, E, I, M, Q** and **U**]. The same cells were also stained for various markers specific for pancreas, PDAC stem cell, or macrophage markers. Panels [**B, C, F** and **G**]: PDAC stem cell marker ALDH1A1 (Green) and pancreas marker ZG16B (red). Panels [**J, K, N** and **O**]: PDAC stem cell marker ALDH1A1 (Green) and pan-macrophage marker CD68 (Red). Panels [**R, S**]: Pancreas marker S100PBP (Green) and PDAC stem cell marker CD44 (Red). Panels [**V, W**]: M2-polarization macrophage marker CD206 (Green) and PDAC stem cell marker CD44 (Red). Composite images are shown in Panels [**D, H, L**, **P, T** and **X**].

https://doi.org/10.1371/journal.pone.0184451.g001

concentrated staining for MIF is actually "extranuclear", within the tunnels or invaginations of cytoplasm). MTFs contained large numbers of mitochondria, lysosomes, autophagic vacuoles, and various autolysomal breakdown products (including laminated bodies structurally comparable to lysosomes), and various structural remnants (Fig 6, Panels G & H). Heterogeneously-sized autophagic vacuoles containing chromatin (and micronuclei) were often a prominent feature, with some very dense remnant bodies (Fig 6H).

Notably, most nuclei also showed focal areas of condensed chromatin by TEM (Fig 6). They characteristically did not show fibrillar centers, or dense fibrillar or granular components generally seen in nucleoli. These regions may represent the ultrastructural correlate of focal areas of condensed "DAPI-intense" chromatin regions which have been reported in fusions between embryonic stem cells and somatic cells [35], and linked to malignancy in prostate cancer [36].

Single cell RNASeq analyses of cultured MTFs

We also performed single cell RNA-Seq expression analyses on cells from 4 patients that both included and excluded assembled transcripts without coding potential (see Materials and Methods for details). Most of the transcripts identified were found in both analyses, although there were a few transcripts of interest which showed up differentially. These notably included CD74 (in the signaling pathway for MIF), which was one of the most highly expressed transcripts across all cells in all patients, as well as a few other genes such as HNRNPA2B1 (see below).

Expression clustering was done using complete linkage clustering with Euclidean distance across individual cells. The analysis that excluded transcripts without coding potential identified 5 clusters, which were common to all 4 patient datasets. Cluster 5 contained only 3 transcripts, all representing Long Interspersed Element-1 (LINE-1) retrotransposons (see below), which curiously encoded only ORF2. However, Cluster 1 also contained 14 distinct LINE1 transcripts, encoding both ORF1 and ORF2, as well as HNRNPA2B1, which is an HNRNP component which positively regulates LINE-1 retrotransposition (see Discussion). LINE-1 retrotransposons form the only autonomously active family of transposable elements [37]. Since the RNA transcripts contained both ORF1 and ORF2, this would appear to indicate that this family is actively engaged in moving DNA elements in these cells.

Cluster 4 contained only 3 transcripts, composed of ferritin light chain (FLT) and ferritin heavy chain (FTH1), which have been associated with several cancers [38–40]. Ferritin has been found in stroma and tumor-associated macrophages in breast cancer [41], where it was associated with increasing grade and stimulated proliferation of breast cancer cells via an iron-independent mechanism. FTH1 also serves as a novel marker for macrophages [42], and FTL is a prognostic marker in tumor-associated macrophages [43], along with CD163. In the analysis which included non-coding transcripts, FTL and FTH1 were present in cluster 2 (see **Table 1**).

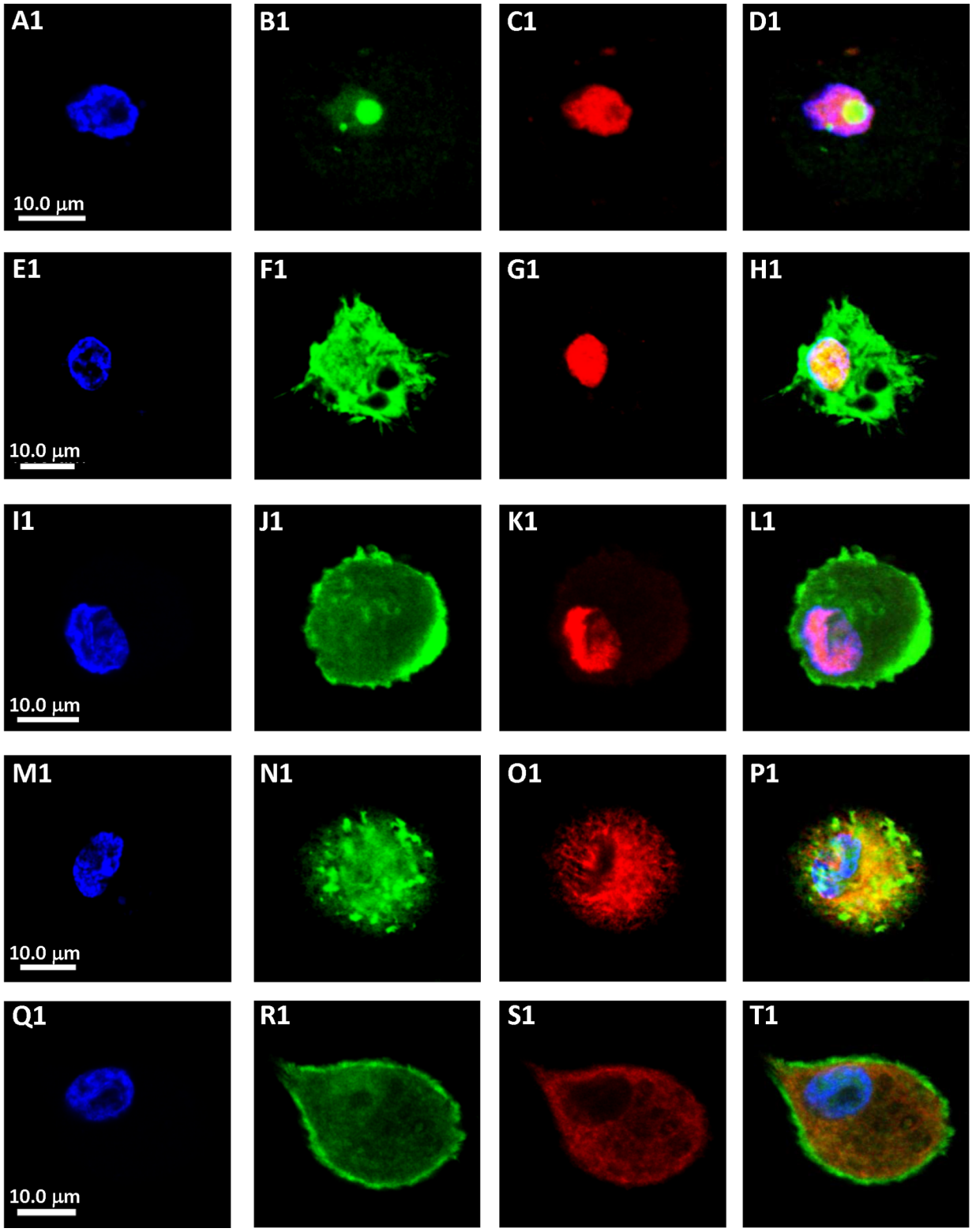
[PDAC MTFs]
A1
B1
C1
D1
10.0 μm
E1
F1
G1
H1
10.0 μm
I1
J1
K1
L1
10.0 μm
M1
N1
O1
P1
10.0 μm
Q1
R1
S1
T1
10.0 μm

Fig 2. Immunostaining of cultured MTFs from PDAC patients. Representative confocal images of cultured MTFs from different PDAC patients. Nuclei were stained with DAPI (Blue) shown in Panels [**A1, E1, I1, M1** and **Q1**]. The same cells were also stained with various fluorescent markers specific for pancreas, macrophage, the pre-carcinogenic cytokine MIF and its receptor CXCR4. Panel [**B1, C1**]: MIF (Green) and pancreas-specific marker ZG16B (red). Nuclei had "tunnels" which were stained strongly for MIF. Panels [**F1, G1, J1** and **K1**]: CXCR4 (Green) and pancreas-specific marker ZG16B (red). Panels [**N1, O1, R1** and **S1**]: CXCR4 (Green) and M2-polarization macrophage marker CD204 (Red). Composite images are shown in Panels [**D1, H1, L1**, **P1** and **T1**].

https://doi.org/10.1371/journal.pone.0184451.g002

The analysis that included non-coding transcripts disclosed 3 clusters that were common to all 4 patient datasets, which we will discuss in more detail (the individual transcripts in the clusters are provided in Supplementary Material; as mentioned, most of the identified transcripts were found in both analyses).

Pathway enrichment analysis using WebGestalt identified a number of KEGG Pathways/ disease categories among the highly expressed transcripts. These included Lysosome, Phagosome, Leukocyte transendothelial migration, regulation of actin cytoskeleton, antigen processing and presentation, NK cell-mediated toxicity, focal adhesion, B-cell receptor signaling, tight junction, osteoclast differentiation, pathways in cancer, bacterial invasion of epithelial cells, prostate cancer, and various infectious categories. The initial analysis identified immunologic diseases, stress, shock, lysosomal diseases, metabolic diseases and neoplasm metastasis, a category which contained 19 genes. However, a closer perusal of the data on a gene-by-gene basis identified a much larger number of genes which are implicated in cancer progression and metastasis (see Table 1). The largest cluster in the analysis that included transcripts without coding potential contained ~ 350 transcripts. It included a number of genes with obvious cancer relevance including CD44, catenin b1 (CTNNB1), vimentin (VIM), cathepsins B and S (CTSB, CTSS), MMP9, XIAP, JunD, numerous proto-oncogenes (REL, YES, SET, FGR, CRK), and HSP90AA1 (which is a chaperone which stabilizes MIF as a client). CD44 was uniformly expressed in all cells from all patients at very high levels; in fact, CD44 expression has been correlated with CD204 expression in PDAC, which serves as a predictor of survival [44].

When the individual genes were examined on a gene-by-gene basis, an additional 64 genes were identified which have been implicated in cancer progression and metastasis, as well as 6 long noncoding RNAs implicated in control of metastasis (see Table 1). For examples, Cathepsins B, D, and S were identified in cluster 3; they have a role in cancer progression and metastasis [45–48]. Nuclear protein 1 transcription regulator (NUPR1, also called candidate of metastasis 1) has been implicated in progression of pancreatic [49], bladder [50], liver [51] and non small cell lung cancers [52]. Nuclear paraspeckle assembly transcript 1 (NEAT-1) is a lncRNA that acts as a transcriptional regulator controlling expression of many genes implicated in progression and metastasis of many cancers [53, 54]. Other genes of interest included DNA damage-regulated autophagy modulator 1 (DRAM1), which plays a major role in regulating autophagic flux including fusion of lysosomes with autophagosomes and clearance of autophagosomes [55]. Also contained in the cluster were a number of macrophage markers (CD68, etc.).

In addition to these coding transcripts, the long noncoding transcript metastasis associated lung adenocarcinoma transcript 1 (MALAT1) was expressed in all cells from all patients. MALAT1 acts as a transcriptional regulator controlling expression of a number of genes involved in metastasis and prognosis in a variety of cancers [56, 57], including lung cancer [58] and in PDAC [59]. In fact, in terms of expression levels, MALAT1 and CD74 were the 6th & 7th most highly expressed transcripts (for reference, mitochondrial 16S rRNA was the most highly expressed transcript, followed by 4 other mitochondrial genes). In addition, all MTFs from one patient highly expressed a novel variant MALAT1 transcript (lacking ~ 300 nt from nt4600-4900, and apparently containing additional 5' and 3' sequences), which could have

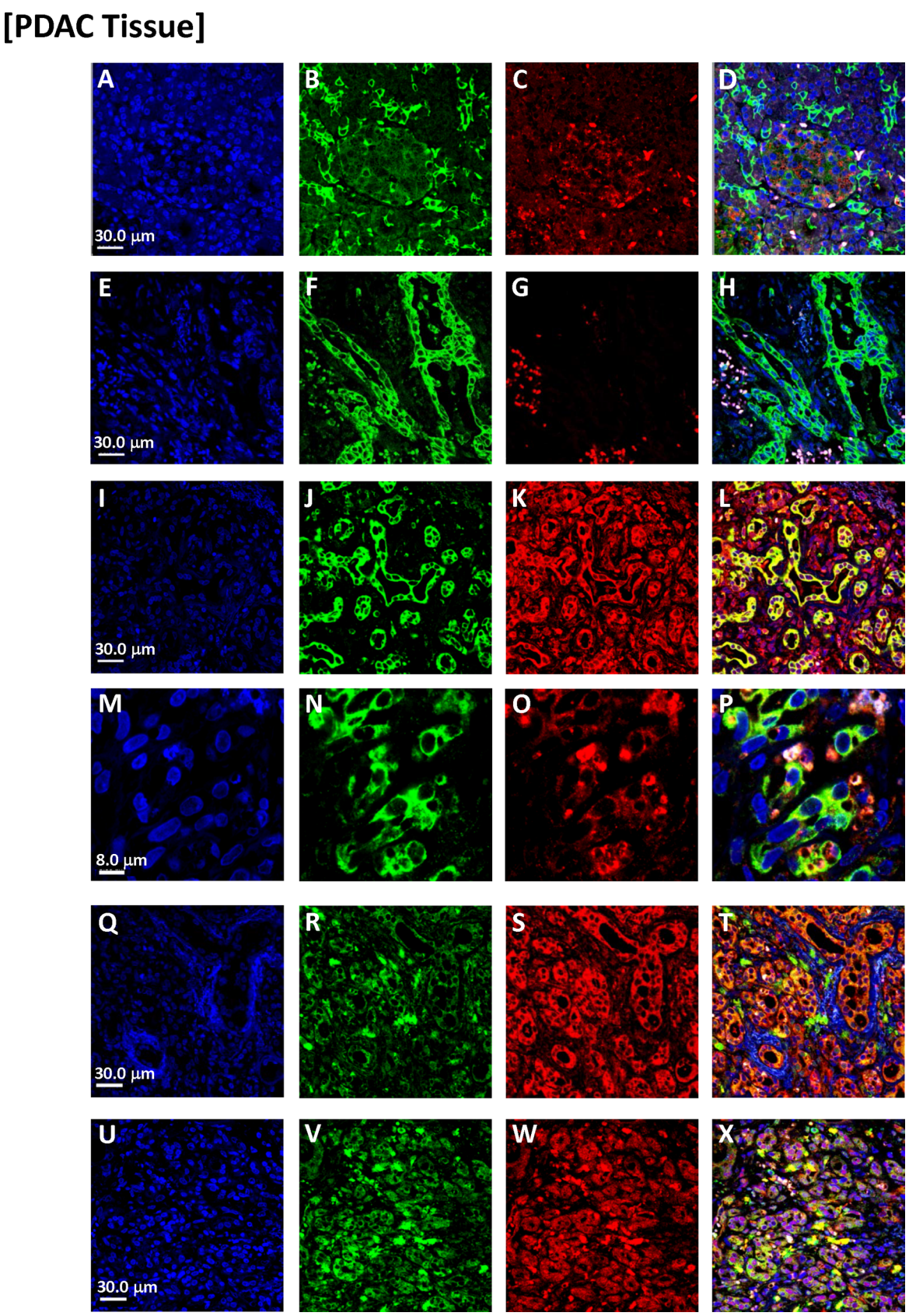
[PDAC Tissue]
A
B
C
D
30.0 μm
E
F
G
H
30.0 μm
I
J
K
L
30.0 μm
M
N
O
P
8.0 μm
Q
R
S
T
30.0 μm
U
V
W
X
30.0 μm

Fig 3. Representative confocal images of MTFs in PDAC tissues from different patients. Nuclei were stained with DAPI (Blue), shown in Panels [**A, E, I, M, Q** and **U**]. The same cells were also stained with various markers specific for pancreas, macrophage, or epithelial differentiation. Panels [**B, C, F** and **G**]: Epithelial marker pan-cytokeratin (Green) and M2-polarization macrophage marker CD206 (Red). Panels [**J, K**]: Epithelial marker pan-cytokeratin (Green) and M2-polarization macrophage marker CD163 (Red). Panels [**N, O**]: Epithelial marker pan-cytokeratin (Green) and M2-polarization macrophage marker CD204 (Red). Panels [**R, S**]: M2-polarization macrophage marker CD206 (Green) and epithelial marker EpCAM (Red). Panels [**V, W**]: M2-polarization macrophage marker CD206 (Green) and pancreas-specific marker ZG16B (Red). Composite images are shown in Panels [**D, H, L**, **P, T** and **X**].

https://doi.org/10.1371/journal.pone.0184451.g003

functional ramifications. Other identified lncRNAs included LUCAT1, which is important in non-small cell lung cancer, NEAT1, and HELLPAR. Two additional antisense RNAs were identified, with cancer relevant sense targets (Table 1).

Dissemination of MTFs after orthotopic implantation into mice

We then performed xenograft experiments, in which cultured MTFs were orthotopically transplanted into mouse pancreas, and mice were necropsied and examined 4, 8, or 12 weeks after transplantation (**Fig 7**). There was no evidence of overt tumors within the pancreata (or any other tissue sites) grossly in any of the animals. Microscopically, there were islands of well-differentiated MTFs within the pancreas, which appeared to be encased within lymphatic channels (Fig 7), at all time points examined. Although the cells were clearly of human origin (based on recognition of multiple markers by human-specific antibodies), they were much smaller and quite uniform in appearance in the pancreatic foci, and thus appeared quite different than when they were grown in culture (this was also true regarding melanoma MTFs). Heterogeneous staining for KRT, CD206, CD204, and ALDH1A1 was observed within the pancreatic foci, as was the case with the well-differentiated islands observed with melanoma cells after subcutaneous transplantation into nude mice [24].

In addition, however, we also observed individual cells (or small clusters of cells) which stained for KRT, or for human antigens ALDH1A1, CD204 and/or CD206 in various other tissues. In animals examined 4 weeks after transplantation, occasional individual cells, or small clusters of cells, showed expression of ALDH1A1 and CD204 in liver parenchyma and in spleen (Fig 7A), where staining was confined to small pericapsular clusters. Individual cells expressing CD204 were observed in focal areas within hepatic parenchyma; in general, their appearance was very similar to surrounding hepatocytes. Curiously, we did not observe staining for CD206 in hepatic parenchyma; however, we did observe individual cells expressing human CD206 in submucosal regions near bile ducts or vessels. Analogous results were also observed in animals sacrificed 8 weeks after transplantation (Fig 7B). At 12 weeks after transplantation, similar well-differentiated focal islands of cells were again observed within pancreas. Individual cells (or small clusters) expressing ALDH1A1 and CD204 were observed in liver and spleen, and occasional cells expressing CD204 were also observed in lung parenchyma (Fig 7C). Individual cells staining positively for CD204 and/or CD206 were also observed in submucosa in various locations (submucosa surrounding bile ducts, small bowel mucosa, etc.).

In general, cells observed in the various tissues were heterogeneous, and often appeared quite large and irregularly shaped. There did not appear to be any obvious progressive increase in numbers of cells over the 4 to 12 week period, although MTFs were only observed in lung after 12 weeks (Fig 7C).

We observed analogous results with immunofluorescent confocal microscopy (**Figs 8 and 9**) for various markers, including KRT, CD206, CD204, CXCR4 and ALDH1A1 (Fig 8 shows pancreas from 8 week animals). Staining for additional human markers S100PBP, CXCR4,

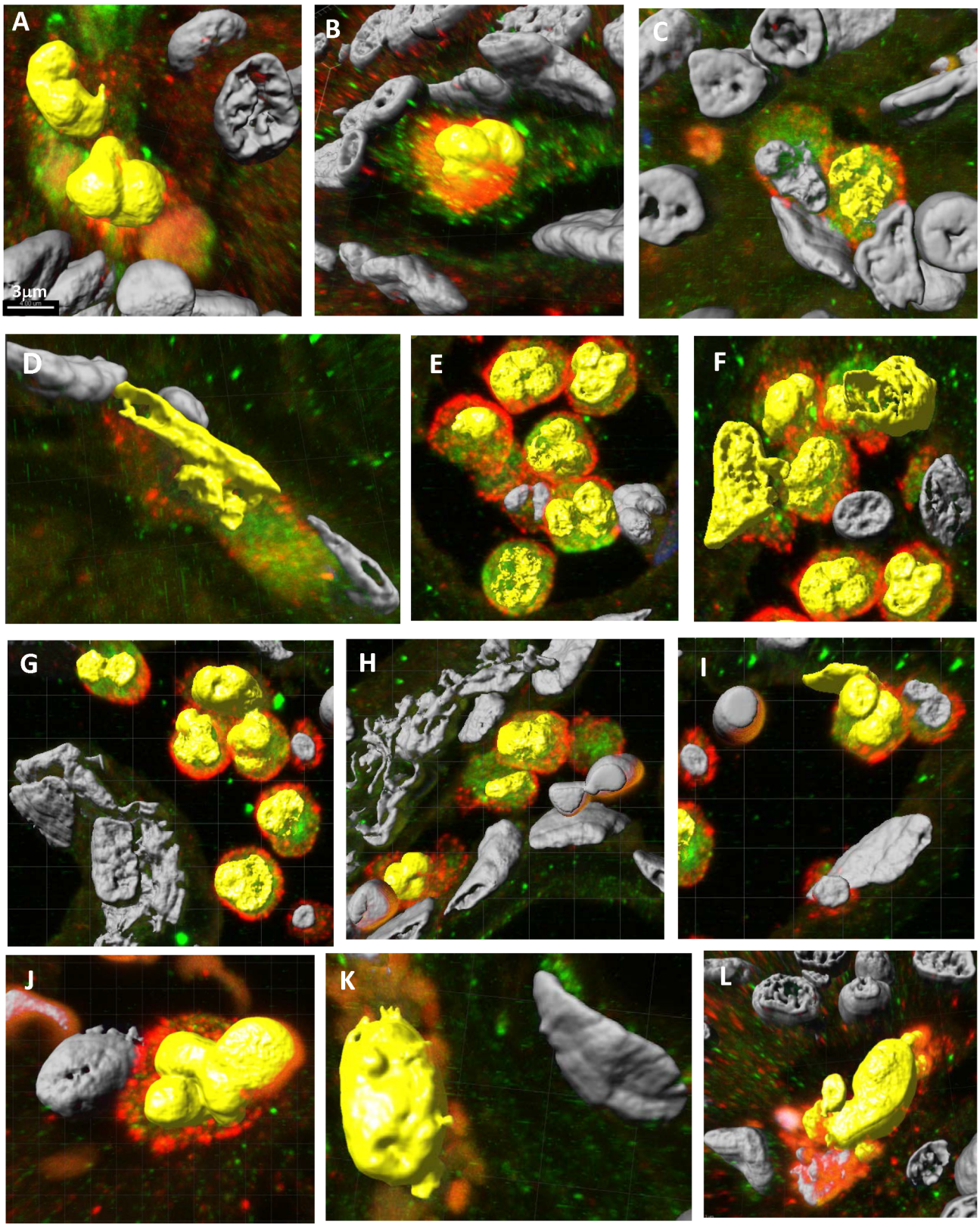

Fig 4. Representative 3D confocal images of MTFs in PDAC tissues from different patients which show various nuclear geometries (Yellow) of dual-stained cells. [Panels **A—I]:** Dual stained for pancreatic tumor marker ZG16B (Red) and macrophage marker CD 206

(Green); [Panels **J & K]:** Dual stained for pancreatic tumor marker ZG16B (Red) and macrophage marker CD 204 (Green); [Panel **L]:** Dual stained for pancreatic tumor marker S100BPB (Green) and macrophage marker CD 204 (Red).

https://doi.org/10.1371/journal.pone.0184451.g004

CD204, and CD206 identified obvious foci in pancreas of animals at 4, 8, and 12 weeks after implantation. We observed dual-staining scattered cells throughout other tissues, including spleen and liver (Fig 9). We also observed dual-staining for human pancreatic and macrophage markers in pancreas (Fig 9), including for S100BPB and ZG16B. No staining was observed in pancreas from control mice (Fig 8).

Discussion

To briefly summarize some aspects of our results, cultured MTFs: 1) Uniformly co-express many epithelial/macrophage/pancreatic stem cell markers; 2) Show ultrastructural features suggestive of functional macrophages, with prominent autophagy; 3) Show high and consistent expression of the CD44:CD74:CXCR4:MIF signaling axis; 4) Show high, and apparently functional, expression of LINE-1 Retrotransposons (along with a positive regulator of their retrotranspositional activity) and the lncRNA MALAT1, based on RNASeq results; and 5) Were capable of "stealth" dissemination in vivo, whereby they metastasized to various distant sites and colonized the sites without forming apparent tumors.

The MTFs characteristically expressed a number of macrophage markers, many of which are characteristic of M2-polarized macrophages, such as CD163, CD204, and CD206. CD163 (Gene ID#9332) is a member of the scavenger receptor cysteine-rich superfamily, which may reflect proinflammatory cytokine production, and there are various reports linking its expression with poor prognosis in various cancers [60, 61]. CD204 (Gene ID#4481 or MSR1, the class A macrophage scavenger receptor type 1) is a functional receptor which mediates the endocytosis of low density lipoproteins, and its expression has also been linked with various cancers as well as with intralymphatic metastasis [62] CD206 (Gene ID#4360, also known as MRC1, the mannose receptor, C type 1) is involved in glycoprotein metabolism, and curiously has also been shown to be involved with CD44 in lymphatic trafficking [63]. We suggest that expression of these receptors may indicate use of alternative energy sources by transformed cells [64–69]. It is also of interest that while PANC-1 human PDAC cells strongly express CD204 and CD206, they do not express pan-macrophage markers like CD68 (Gene ID#968) or CD14 (Gene ID#929): CD68 and CD14 are unlikely to contribute to altered metabolic requirements.

The M2-polarization of cultured MTFs may have significant ramifications. M2-like macrophages are responsible for collagen degradation through a mannose receptor-mediated (CD206) pathway [70], and tumor associated macrophages (TAMs) generally acquire an M2-like phenotype that plays important roles in many aspects of tumor growth and progression [71–74], and M2-polarized TAMs have also been found to promote the EMT in various carcinomas [75, 76].

In fact, there are a growing number of reports of expression of macrophage markers on various types of cancer cells. For example, CD163 expression on rectal cancer cells is associated with early local recurrence and reduced survival time [77]. CD163 expression by breast cancer cells is related to early distant recurrence and reduced survival time [78]. In this regard, Shabo & Svanvik [79] reported that ~50% of breast cancer cells expressed CD163, and that a third of rectal cancer cells expressed it. CD163 was again associated with early distant recurrence in breast cancer, and with local recurrence in rectal cancer, and with reduced survival times in both. Expression of DAP12, a macrophage fusion receptor, was also associated with advanced

[PDAC Ploidy Data]

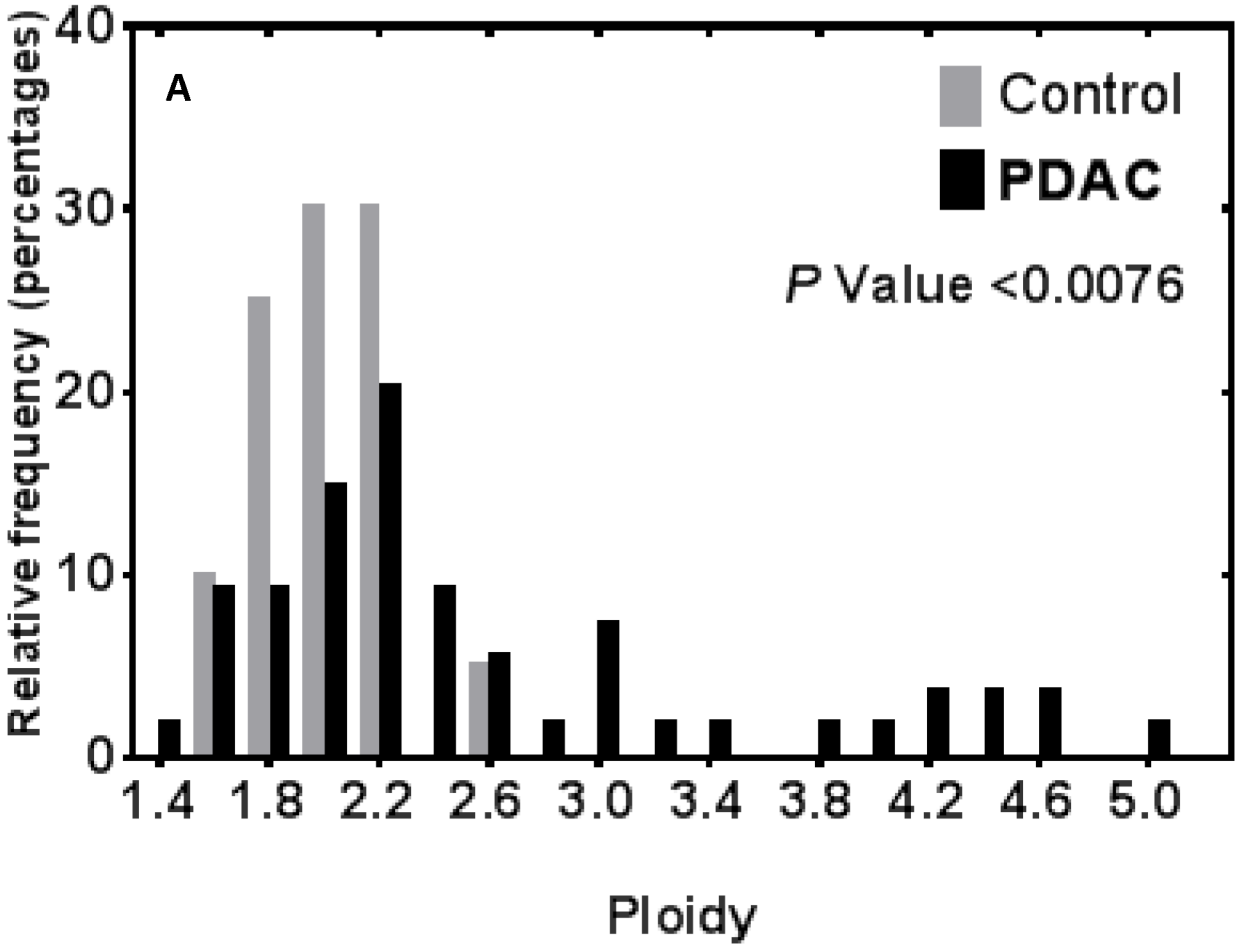

Fig 5. Ploidy analysis of dual-staining MTFs in PDACs. DNA content analysis of dual-staining cells was performed as described in PDACs in archival FFPE tissues. DNA content was also analyzed in adjacent "normal" pancreas (gray bars). Populations of MTFs from 2 patients, showed cells with DNA distribution peaks corresponding to "para-diploid" but with many aneuploidy cells distributed throughout the range, including some with DNA contents ranging up to 5n (black bars).

https://doi.org/10.1371/journal.pone.0184451.g005

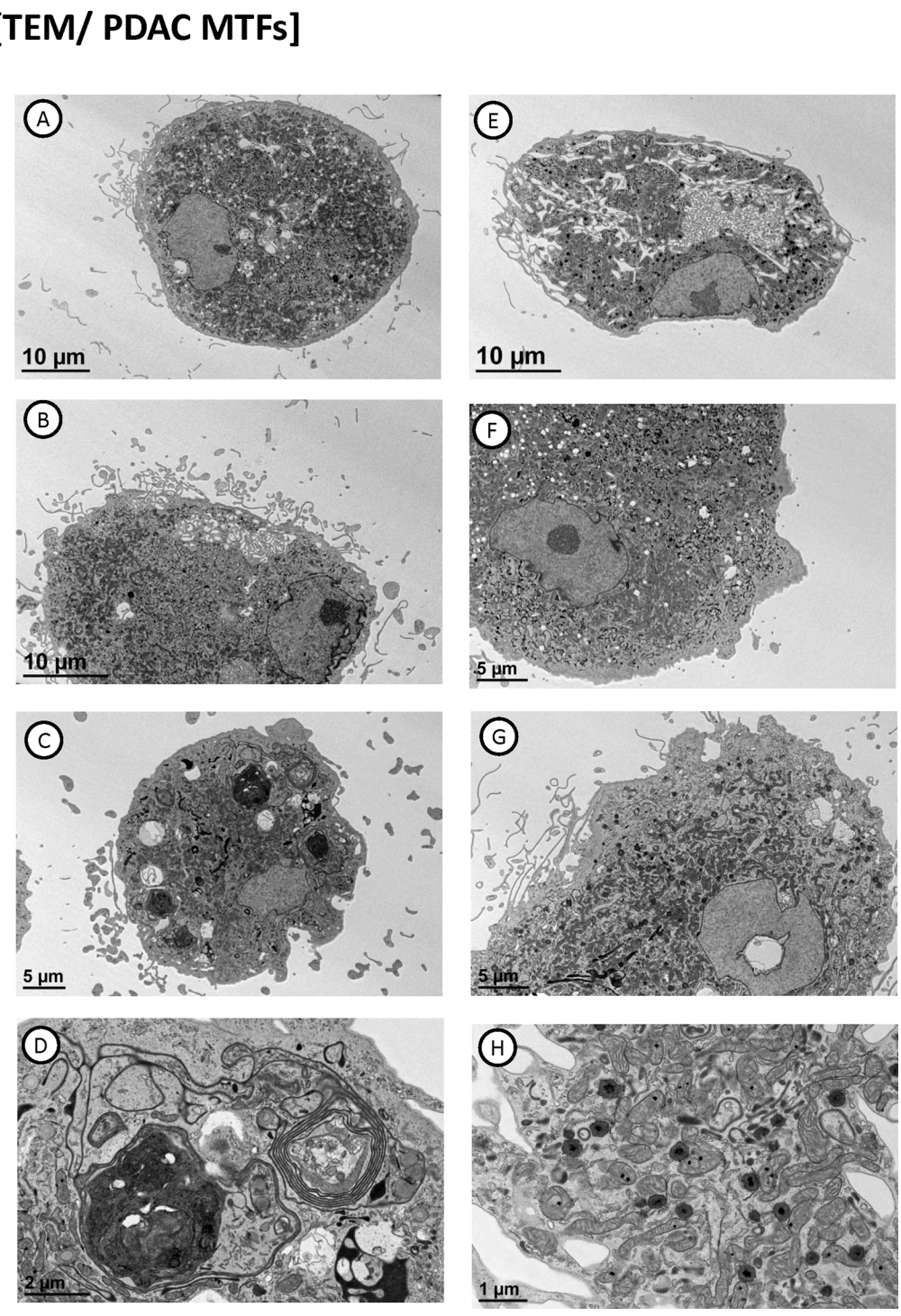

Fig 6. Transmission electron microscopy of cultured MTFs. Panels **A-H** show representative cells with distinctive features, including cytoplasmic "tunnels" through nuclei (Panel **G**). Focal hyper-dense regions of chromatin (Panel **A**, **E**, and **F**), autophagic bodies (Panel **D**), etc. are evident within the individual cells.

https://doi.org/10.1371/journal.pone.0184451.g006

tumor grade and higher rates of skeletal and liver metastasis, and overall shorter distant recurrence-free survival.

Table 1. Cancer-related genes of interest.

Cluster 1		Cluster 2		Cluster 3	
Gene Name	**Reference(s)**	**Gene Name**	**References**	**Gene Name**	**Reference(s)**
PAG1	[132–134]	NANOG	[135]	TMSB10	[136–138]
ENO1	[139–141]	GPNMB	[142]	CTSD	[46]
CD38	[143–146]	ITGAX	[147]	CTSB	[47, 48]
EREG	[148, 149]	FTH1	[38–41, 43]	CTSS	[45]
DRAM1	[150–152]	FLT	[38–41, 43]	GPNMB	[142]
IREB2	[153, 154]	FUCA1	[155, 156]	S100A6	[157–160]
PEBP1	[161–164]	TMSB4X	[165, 166]	ANXA2	[167–169]
PTPN3	[170]	NABP1	[171, 172]	NBPF10	[173–175]
ARCN1	[176]	MALAT1 (lncRNA)	[56–59]	NEAT1 (lncRNA)	[54, 177–180]
NCOR1	[181]	CTSB	[47, 48]	HELLPAR (lncRNA)	[182]
SNRPD1	[183]				
DPYSL2	[184, 185]				
SRRM1	[186]				
NUPR1	[50–52]				
C16orf72	[187]				
HMGB1	[188]				
MGAT1	[189]				
HMGB1	[190–192]				
PARD6G	[193]				
ICK	[194, 195]				
ELK4	[196, 197]				
SIRPA	[198, 199]				
NUCKS1	[200–202]				
NUAK2	[203, 204]				
PYHIN1	[205]				
LAMP2	[206, 207]				
B4GALT5	[208–210]				
PRDX1	[211]				
TSPAN14	[212]				
CAP1	[213–216]				
DFFA	[217]				
HAUS2	[217, 218]				
MOB1A	[219]				
ITGB2	[220, 221]				
ST3GAL1	[222–224]				
ROCK1	[225–227]				
NIT2	[228]				
TFRC	[229]				
PTMA	[230]				
GPNMB	[142]				
CAPG	[231, 232]				
DDX51	[233]				
TFRC	[234]				
TRA2B	[235–237]				
SGK1	[238]				
S100A11	[239, 240]				

(*Continued*)

Table 1. (*Continued*)

Cluster 1		Cluster 2		Cluster 3	
Gene Name	**Reference(s)**	**Gene Name**	**References**	**Gene Name**	**Reference(s)**
ACTR3B	[241]				
LSP1	[242–244]				
HERC4	[245]				
DOCK8	[246, 247]				
ANAPC15	[248]				
GINS4	[249, 250]				
SLC1A5	[251, 252]				
PTPN2	[253, 254]				
ADGRE2	[255, 256]				
GALNT6	[257, 258]				
MARCKS	[259–263]				
DIXDC1	[264]				
NBPF10	[173–175]				
TP53					
PHLDB1	[265, 266]				
PHACTR4	[267]				
ASAH1	[268–270]				
CCNI	[271, 272]				
Long noncoding RNAs					
NEAT1	[54, 177–180]				
LUCAT1	[273–275]				
MALAT1	[56–59]				
HELLPAR	[182]				
DDR1-AS1	[276, 277]				
KCTD21-AS1	[278]				

https://doi.org/10.1371/journal.pone.0184451.t001

After orthotopic implantation in mice, the cultured MTFs were able to disseminate widely to various tissues, including (at least) pancreas, spleen, liver, and lung. They colonized the distant sites generally as single cells. After dissemination, some of the MTFs did not appear to continue to express all of the macrophage markers they expressed in primary cultures, and at times displayed some apparent plasticity in their morphology. For example, discordant expression of the CD204 and CD206 markers was observed in liver. Staining for CD204 was positive within hepatic parenchyma for individual cells and focal nests of cells in liver of animals at 4,8, and 12 weeks after transplantation (Fig 7). These positively staining cells were observed only in select regions of the livers, and they appeared as well-differentiated cells morphologically similar to hepatocytes. However, staining for CD206 was not observed in hepatic parenchyma at any of the time points. Scattered cells staining positively for CD206 were observed in submucosa of vessels and bile ducts (see Fig 8A and 8C); these cells were large, irregularly shaped cells with morphology more consistent with macrophages, which was also evident in confocal micrographs in pancreatic foci (Fig 8).

Ding et al. [80] reported that MTFs may acquire cancer stem cell properties in breast cancer cells. They noted expression of CD163 in breast cancer tissues, where it varied significantly and CD163 expression correlated with ER expression. These investigators created fusions between M2-polarized macrophages and breast cancer cell lines. The MTFs gained a $CD44^{+}CD24^{-/low}$ phenotype, overexpressed EMT related genes, and showed

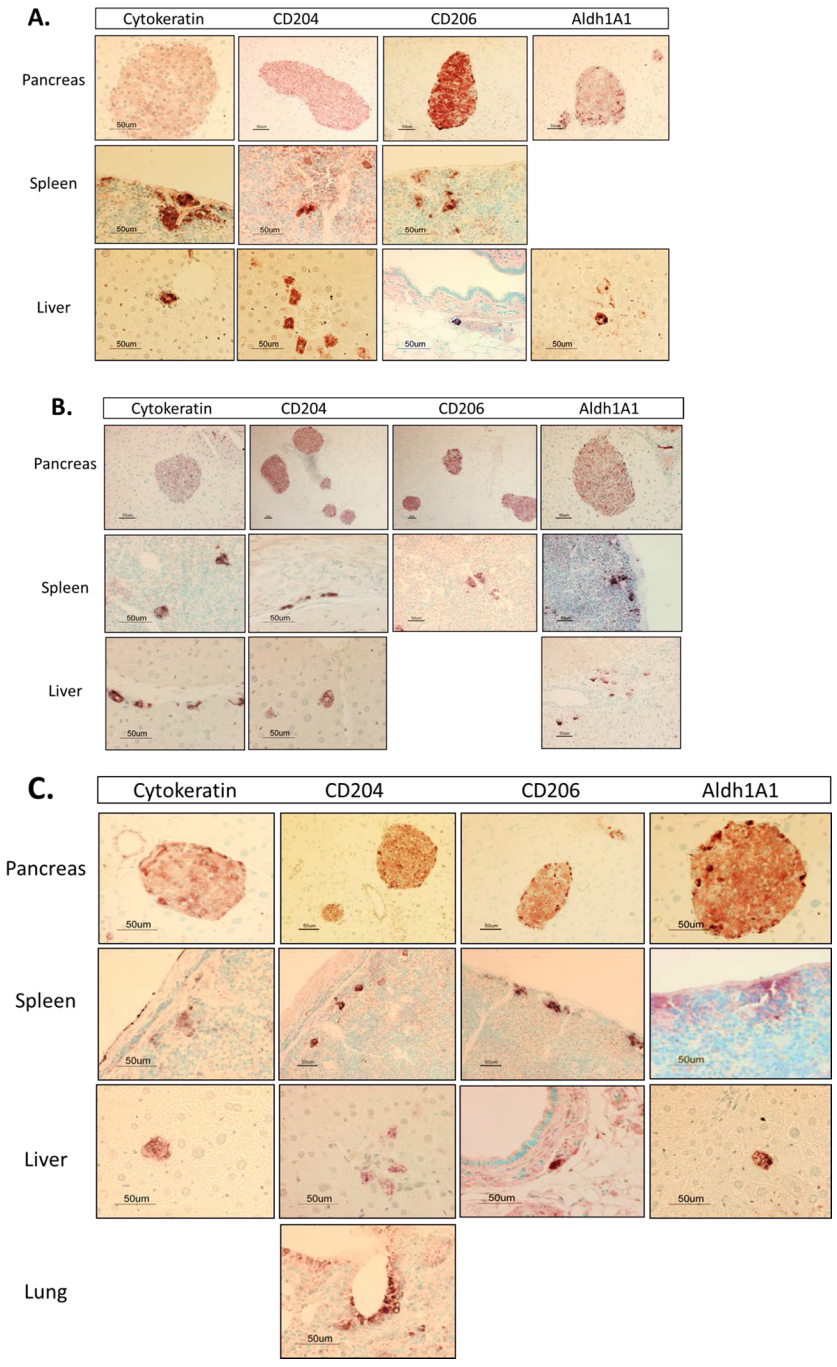

Fig 7. Immunohistochemical staining of mouse tissues after orthotopic transplantation of cultured MTFs. Human MTFs were cultured from blood as described, and orthoptically transplanted into mouse pancreas. After various periods of time, tissues were harvested and stained for an epithelial marker (cytokeratin, KRT), human macrophage M2 polarization markers CD204 and CD206, and human pancreatic stem cell marker ALDH1A1. Tissues (pancreas, spleen, and liver) are as indicated. Panel **A** shows samples harvested at 4 weeks after implantation, **B** shows samples after 8 weeks, and **C** shows samples after 12 weeks.

https://doi.org/10.1371/journal.pone.0184451.g007

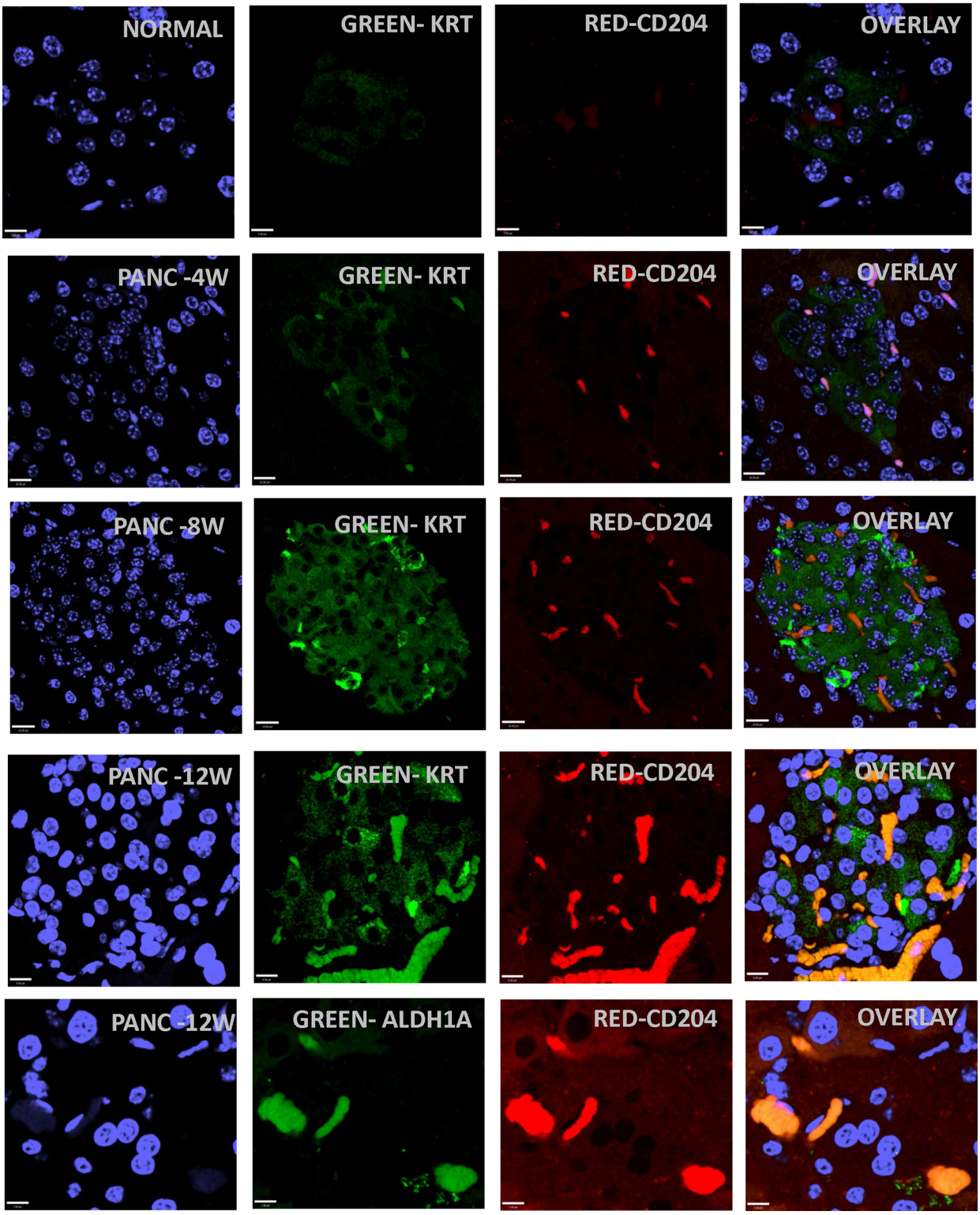
[PANC1/ IHF]
NORMAL
GREEN- KRT
RED-CD204
OVERLAY
PANC -4W
GREEN- KRT
RED-CD204
OVERLAY
PANC -8W
GREEN- KRT
RED-CD204
OVERLAY
PANC -12W
GREEN- KRT
RED-CD204
OVERLAY
PANC -12W
GREEN- ALDH1A
RED-CD204
OVERLAY

Fig 8. Immunostaining of human MTFs after orthotopic transplantation into mice. Cultured human MTFs were orthotopically transplanted into mouse pancreas and tissues were harvested at various times. Representative confocal images are shown from pancreas after 4, 8 and 12 weeks (**PANC-4W, PANC-8W, PANC-12W**) after orthotopic implantation. Nuclei were stained with DAPI (Blue). The same cells were also dual stained with various fluorescent markers specific for the epithelial marker cytokeratin (**KRT**), human macrophage M2 markers (**CD204/206**) or the human pancreatic stem cell marker (**ALDH1A1**).

https://doi.org/10.1371/journal.pone.0184451.g008

increased migration, invasion, and tumorigenicity (but reduced proliferation). There was some indication that the fusions were also associated with increased metastasis, although an increase in metastases was also observed with mixtures of the M2-differentiated U937D cells and breast cancer cell lines (both MCF7 and MDA-MB-23) without fusion, so the role or occurrence of fusion per se was not clear. The cultured MTFs described here appear to mirror these properties.

MIF in the TME and cancer progression

We also observed activation of the MIF signaling axis in the cultured PDAC MTFs. MIF has important roles in the TME as well as progression of many cancers. MIF levels are associated

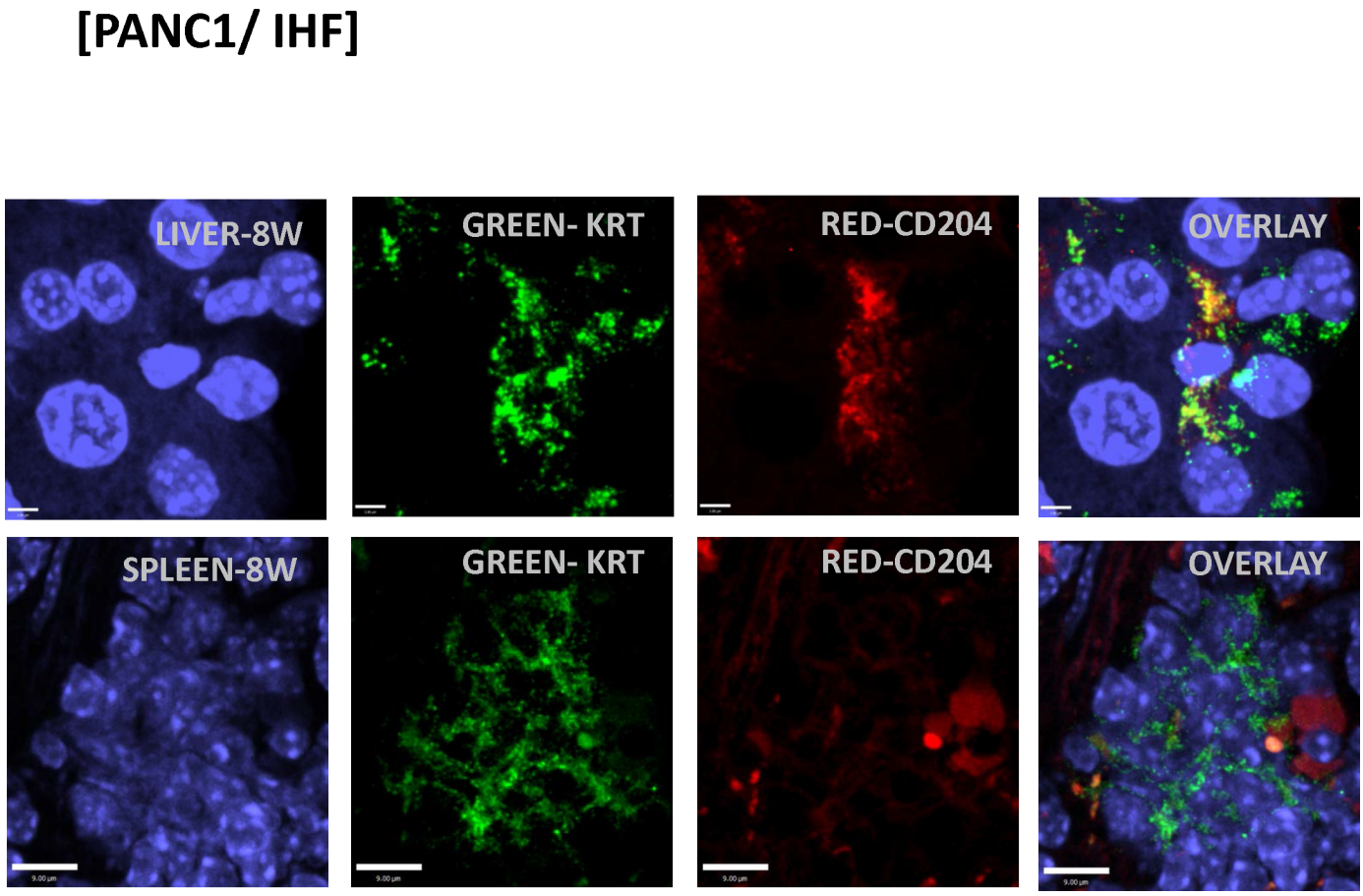

Fig 9. Immunostaining of human MTFs after orthotopic transplantation into mice. Cultured human MTFs were orthotopically transplanted into mouse pancreas. At 8 weeks following implantation, tissues were harvested and examined by confocal microscopy. Representative confocal images of liver or spleen (**LIVER-8W, SPLEEN-8W**) are shown. Nuclei were stained with DAPI (Blue). The same cells were also dual stained with various fluorescent markers specific for epithelial marker cytokeratin (**KRT**) or macrophage (**CD204/206**). Note that the CD204-expressing cell is no longer expressing KRT.

https://doi.org/10.1371/journal.pone.0184451.g009

with an increased incidence of a large number of cancer types [28, 32, 81–86]. MIF serves as a non-cognate ligand for CXCR4 [32, 33]: MIF (and CXCR4) in the TME are adverse prognostic indicators [28], and it can induce CXCR ligand and regulators of macrophage infiltration, especially CD44 [87]. In PDAC, MIF has been shown to induce the EMT [88, 89], enhance tumor aggressiveness, and predict clinical outcome in resected PDACs [27]. M2 polarized TAMs also have prognostic importance in PDAC [73, 90], and targeting TAMs decreases tumor-initiating cells, relieves immunosuppression, and improves chemotherapeutic responses [91]. MIF controls alternative activation of TAMs to M2-polarization [88]; In turn, co-culturing M2-polarized TAMs with PDAC cells strongly induces the EMT [89].

MIF expression is up-regulated during hypoxia via an HRE found in the 5'-UTR of the gene [92, 93]. Proteomic and tissue array profiling has identified elevated hypoxia-regulated proteins in microdissected PDAC nests vs. normal ducts [94], prominently including MIF, which showed excellent ROC curves in discriminating PDACs from non-malignant lesions. MIF is a direct transcriptional target of HIF1a, and loss of MIF results in inefficient HIF1a stabilization induced by hypoxia [95]. In this context, CSN5 of the COP9 signalosome interacts with MIF in PDAC cells to stabilize HIF1a. Intracellularly, MIF is also stabilized by complexing with HSP90 chaperone [83, 86], which was found in cluster 2 in the RNASeq data analysis (Cluster 2 also contained CD74). Cancer cells contain constitutive endogenous MIF-HSP90 complexes, and inhibition of HSP90 function results in apoptosis, which can be overridden by ectopic MIF expression. In fact, the metastasis-promoting CD44 in PDACs is actually the signaling component of the MIF-CD74 receptor complex [34]. MIF signaling through CD74 promotes sustained ERK activation, which corresponds to the main outcome from Ras mutations, mutations which figure so prominently in PDAC (see [96]). Inhibition of MIF using siRNAs leads to apoptosis in PDAC cells [97]. Long et al. [98] developed a unique mouse model for PDAC lymphatic metastasis. They developed a subline from the BxPC-3 PDAC cell line via serial passages in nude mice. The subline showed increased migration, invasion, and invasive ultrastructural characteristics. Metastasis-related gene alterations found in the subline were very limited but included up-regulation of MIF. We speculate that MIF expression in distant tissues by disseminated MTFs may prepare "niches" for subsequent colonization by metastasis-initiating cells.

CTCs in PDAC

CTC isolation and analysis has become an active area of translational cancer research [99]. However, unlike breast, prostate and lung cancers, comparatively little is known about CTCs in pancreatic cancer, although some literature is appearing [2, 3, 100]. Recent literature using a novel KPCY mouse strain (KPC mice with the addition of a $Rosa^{YFP}$ allele) demonstrated that PDAC cells enter the bloodstream unexpectedly early, during the pre-cancerous PanIN lesion stage and before carcinoma was evident. The circulating, pancreas-derived cells exhibited a mesenchymal phenotype (although somewhat different from that described by Ting et al. [100]), and the number of circulating cells was increased in the presence of chronic pancreatitis [101]. The murine study was recently followed up by a prospective human study that captured circulating cells of pancreas-derived lineage from the blood of patients with pre-cancerous pancreatic lesions but no clinically detectable cancer. Since pancreas-derived cells were present in the blood even at pre-cancerous stages, the authors suggested that these cells could initiate metastatic lesions [102], although many aspects remain unclear. When patient populations with no cancer, pre-cancerous lesions or confirmed carcinoma were compared, the number of circulating, pancreas-derived cells significantly increased with disease progression. These results, as well as other studies [2], provide evidence that cells of pancreatic origin are released into the bloodstream at

significantly earlier stages of tumor formation than previously thought. We point out that these cells could well include MTFs.

Ploidy in PDAC

Here we found that apparent MTFs were a prominent component in human PDACs, and that they specifically show a wide range of aneuploid DNA content (Fig 5), with a large proportion of the cells containing greater than 3n. DNA index is known to be a strong prognostic factor in PDAC patients [103, 104] where 50–75% of patients showed non-diploid DNA contents. There is also a clear relationship between DNA content and survival in PDAC patients. Lymph node involvement was seen in 36% of patients with diploid tumors, vs. 79% of those with aneuploid tumors. 32% of patients with a diploid tumor survived at least 1 year, whereas none of the patients with aneuploidy tumors did [105], and aneuploidy showed a significant association with decreased cumulative survival. Tsavaris et al. [106] found that PDAC patients with ploidy score greater than 3.6 had 5X higher probability of death within a given time-frame compared with patients with ploidy score of less than 2.2, and those with an intermediate ploidy score (2.2–3.6) had a 6.3X higher probability of death compared with patients with ploidy score less than 2.2. A similar relationship was found for patients with late stage colorectal cancers [107]. Given that apparent MTFs appear to constitute a considerable portion of PDAC populations, these relationships may reflect higher MTF proportions.

DNA reconciliation and mobile elements in MTFs

When fusion of 2 different cell types occurs, two distinct cellular programs need to be merged. This process has been referred to as symphiliosis, the process of intracellular reconciliation [108], which suddenly produces new clones with emergent phenotypes. Cancer cells can transduce adjacent TME cells in vivo, and it has been suggested that in vivo fusion discloses genes implicated in tumor progression [109]. Here, we note that the MTFs present a surprisingly uniform immunophenotypic profile, in spite of the often huge differences in DNA content. They appear to be undergoing cellular reconciliation, with prominent autophagy including nucleophagy [110] within autophagosomes which have sequestered chromatin and even micronuclei. Many aspects of micronuclei formation have been detailed [111], and degradation of micronuclei via autophagosomes has previously been reported [112], where it was speculated that removal of micronuclei may contribute to the genome-stabilizing effects of autophagy. Nucleophagy has been reported in various laminopathies [113] and seems to be beneficial for cell survival [113, 114]. The defacto depolyploidization process seems to involve macroautophagy-aided elimination of chromatin, which somehow includes sorting out what will be eliminated.

An additional finding of significance was the uniform expression of various LINE-1 retrotransposons, as well as a positive regulator (HNRNPA2B1) of their expression. Cluster analysis disclosed a considerable number of Long Interspersed Element-1 (LINE-1), some of which included both ORF1 and ORF2. LINE-1 retrotransposons form the only autonomously active family of transposable elements [37], and specific classes of LINE-1 elements are up-regulated during reprogramming and in transformed cells [115]. Since the RNA transcripts contained both ORF1 and ORF2, this would appear to indicate that this family is actively engaged in moving DNA elements in these cells, which presumably comprises part of the "reconciliation" of DNA. Activation of LINE-1 retrotransposons has also been linked to metastasis and the EMT [116].

We note here that most (but not all) of the patient samples analyzed here were relatively late stage PDACs. Although literature clearly suggests that CTCs (and/or MTFs) should be

present in the circulation in early stage disease, this needs to be established before potential therapies targeting circulating MTFs could be deployed to block metastatic spread. We are currently working on PDAC MTF-targeted nanoliposomal delivery of an HSP90A inhibitor, with the goal of eliminating MIF and its signaling axis.

Materials and methods

This Human Subjects Research was approved by the Pennsylvania State University/Hershey Medical Center IRB, and informed written consent was obtained from all participants. Peripheral blood (10–15 ml) was obtained from ~20 patients with pancreatic ductal adenocarcinoma (plus healthy volunteers). Our patient population is ~ 10% Hispanic or Latino, with ~ 10% Black or African American, with a targeted enrollment of 50% male/female.

Isolation and culturing of MTFs

An initial CTC enrichment was performed using Oncoquick porous membrane gradients as previously described [24, 117], or using Ficoll-Paque PLUS gradients (GE Healthcare). The CTC-enriched fractions were rinsed in PBS, and then plated onto standard culture dishes and cultured in RPMI 1640 + 10% bovine serum. After 24 hours, plates were carefully rinsed to remove non-adherent cells, and new medium was added and cultures were continued for various periods of time. The cells appeared large and "epithelioid" at 24 h, and retained the same basic morphology throughout culturing; this was also noted in a previous publication which also examined CTCs captured on filters [117]. Cultures were generally grown for 4–6 weeks, initially in 25 cm plates and later in 75 cm plates. No cells grew in cultures of peripheral blood obtained from normal volunteers.

Immunofluorescent staining of MTF cultures and PDACs

After various culture times, cells were transferred to chamber slides, and after growth for 24 h Immunochemical staining was performed for a variety of different markers (see Table 2).

Fluorescently-labeled secondary antibodies used for the different primary antibodies were purchased from Enco Scientific Services Limited: They included (as necessary):

115-545-062, Alexa Fluor 488-AffiniPure Goat Anti-Mouse IgG; 115-585-062, Alexa Fluor 594-AffiniPure Goat Anti-Mouse IgG; 305-545-003, Alexa Fluor 488-AffiniPure Rabbit Anti-Goat IgG; 305-585-003, Alexa Fluor 594-AffiniPure Rabbit Anti-Goat IgG; 711-545-152, Alexa Fluor 488-AffiniPure Donkey Anti-Rabbit IgG; or 711-585-152, Alexa Fluor 594-AffiniPure Donkey Anti-Rabbit IgG.

Generally, cells were stained for various combinations of 2 markers, as well as DAPI, and examined by confocal microscopy. PANC-1 (ATCC, CRL-1469) cells were also examined in parallel. Controls included no primary antibody as well as normal tissues.

For cultured MTFs, cells were grown overnight in 8-well coated chamber slides (Lab-Tek II CC^2) and immunostaining was performed as previously described [24, 117]. Blocking was performed in PBS + 1:50 dilution of serum (from the species the secondary antibody was produced in) for 1 h at room temperature (RT). 200 microliters/chamber well of primary antibody solutions (1:200 dilution) was used. The balance of the staining protocol was performed in the dark, or with slides protected from light. 200 microliters of secondary antibody (1:500 dilution in blocking solution) was used. To counterstain nuclei, 200 microliters of DAPI solution (1:30,000 in PBS) was added to each well, and incubated for 5 min at RT in the dark. Cells were again washed 3X for 3 min each in PBST, and then a final rinse for 10 min at RT with PBST, and the final wash was again removed by inversion wicking. Coverslips were mounted using 3 drops of ProLong Gold Antifade mounting medium (Invitrogen), pre-warmed to RT, and slides were

Table 2. Antibodies used for immunophenotypic characterizations.

Antigen	Company	Source	Specificiy
ALDH1A1	Santa Cruz Sc22588	Goat polyclonal	human
CD44	R & D Systems Mab7045	Mouse monoclonal	human
CD68	Abcam Ab955	Mouse monoclonal	human
CD163	Abcam Ab87099	Mouse monoclonal	human
CD163	AbD SeroTec MCA1853T	Mouse monoclonal	human
CD204/MSR1	Sino Biological 10427	Mouse monoclonal	human
CD206/MRC1	AbD Serotec MCA2155T	Mouse monoclonal	human
CXCR4	Abcam AB181027	Rabbit polyclonal	human/mouse
CXCR4	Abcam Ab1670	Goat polyclonal	human/mouse
EpCAM	EMD Millipore OP-187	Mouse monoclonal	human
EpCAM	Cell Signaling Tech	Mouse monoclonal	human
MIF	Santa Cruz Sc-20121	Rabbit polyclonal	human/mouse
S100PBP	Atlas Antibodies HPA027328	Rabbit polyclonal	human
Pan-KRT	Santa Cruz Sc-15367	Rabbit polyclonal	human/mouse
ZG16B	R & D Systems Mab7777	Mouse monoclonal	human

https://doi.org/10.1371/journal.pone.0184451.t002

stored in the dark at 4 C. The mounting medium minimizes the refractive index mismatch of the lens immersion liquid (Cargile oil, refractive index of 1.52).

In addition, slides from formalin-fixed paraffin embedded (FFPE) primary human PDAC tumors were also stained for the various markers as described.

Subcutaneous implantation of cultured human MTFs into athymic mice

All animal studies were performed under protocols approved by the PSU IACUC.

Male, 6-week old athymic (nu/nu) mice were purchased from Charles River. For surgical implantation of human PDAC CTCs, animals were fully anesthetized with Ketamine-Xylazine (120 mg/kg—4 mg/kg, i.p.), an incision was made on the left flank and the pancreas was exteriorized. Cultured CTCs from individual PDAC patients, 1.5 x 10^5 cells in 50 microliters of HBSS (n = 3 mice / patient sample) were injected into the pancreas. The incision was closed with surgical wound clips and the animals were monitored for any ill effects. Experiments used cultured MTFs from a number of separate PDAC patient samples, which had been grown in culture for about 4 weeks. Mice were monitored for any outward sign of tumor formation, and they appeared normal throughout. At 4, 8, or 12 weeks after transplantation, mice were fully anesthetized with Ketamine–Xylazine and euthanized by CO_2 administration and cervical dislocation. Lungs, liver, spleen, and pancreas were excised and fixed in 10% neutral buffered formalin for 24 hrs. After equilibration in 70% ethanol, tissues were embedded in paraffin and

sectioned. Hematoxylin/eosin staining and immunohistochemical staining for various human macrophage, pancreatic and epithelial cell markers was done on serial tissue sections.

Tissue specimens from xenografted mice were also stained for the macrophage, stem cell, and epithelial markers (and DAPI) described above, generally using antibodies specific for the human antigens, and examined via IHC and/or confocal microscopy. These included sections from FFPE blocks of various tissues from the mice (liver, lung, pancreas, spleen). In addition, immunohistochemistry was also performed on the various tissues, using multiple antibodies which were specific for the human antigens. For these studies, secondary antibodies and reagents for immunoperoxidase staining were purchased from Vector Laboratories (ImmPRESS Anti-rabbit Ig (peroxidase) MP-7401, and ImmPRESS Anti-mouse Ig (peroxidase) MP-7402). Peroxidase substrate studies used ImmPACT DAB Substrate Kits (SK-4105). Controls included staining of normal mouse tissues as well as no primary antibody.

3D confocal microscopy, image acquisition, and image processing

Confocal images of fluorescently labeled cells were acquired with a Leica AOBS SP8 laser scanning confocal microscope (Leica, Heidelberg, Germany) using a high-resolution Leica 40X/1.3 Plan-Apochromat oil immersion objective. The laser lines used for excitation were continuous wave 405 (for DAPI), 80 MHz pulsed 499 nm (for Alexa 488), 80 MHz pulsed 591 (for Alexa 594). These laser lines were produced by UV diode, 80 MHz white light laser (Leica AOBS SP8 module) respectively and the respective emission signals were collected sequentially using AOBS tunable filters as follow; 410–480 nm for DAPI (this exclude possible RNA bound DAPI emission which occurs above 500 nm), 504–571 nm for Alexa 488, 597–751 nm for Alexa 594 and 650–790 nm for TO-PRO-3. All images, spectral data and DNA ploidy measurement data were generated using the highly sensitive HyD detectors (with time gated option) in descanned mode and the photon counting mode was particularly used for collecting signals from DAPI for DNA ploidy measurements. The backscattered emission signals from the sample were delivered through the AOBS tunable filter (to remove irradiated laser), the detection pinhole set to 1 Airy unit (to obtain optimal lateral and axial resolutions), spectral dispersion prism, and finally to the HyD detectors. The width of the slits in front of each HyD could be software adjusted so that each HyD could detect spectral regions spanning from a 10-nm bandwidth up to the overall spectral capacity of the system (400–800 nm). Using this unique option, spectral scanning was per- formed on all the dyes to confirm signal specificity.

For 3D image data set acquisition, the excitation beam was first focused at the maximum signal intensity focal position within the sample and the appropriate HyD gain level was then selected to obtain the pixel intensities within range of 0–255 (8-bit images) using a color gradient func- tion. Later on, the beginning and end of the 3D stack (i.e. the top and the bottom optical sec- tions) were set based on the signal level degradation. Series of 2D Images for a selected 3D stack volume were then acquired with 1024X1024 pixels and were line averaged 3–4 times depending on the noise level. The 3D stack images with optical section thickness (z-axis) of approximately 0.3 micrometers were captured from cell volumes. For each cell volume reported here, z- section images were compiled and finally the 3-dimensional image restoration was performed using Imaris software (Bitplane).

Preparation of MTF cultures for TEM

Cells were grown in culture as described, and then transferred to coverslips (Thermanox cover- slips, 15 mm D, Cat#72275–01) and grown for 3 additional days. Cells were then washed with ice cold 0.1 M sodium cacodylate (NaCAC)buffer, pH 7.3 three times for 5 min. Cells were fixed for 1 h at 4 C in 0.5% glutaraldehyde and 4% paraformaldehyde buffered with

0.1 M NaCAC buffer. They were again rinsed 3X with 0.1 M NaCAC at 4 C, and then post-fixed in 1% osmium tetroxide/1.5% potassium ferrocyanide overnight at 4 C in a wrapped container. Preparations were then rinsed with buffer, dehydrated in a graded series of ethanol, and embedded in Embed 812 (Electron Microscopy Sciences). A diamond knife mounted in a Porter-Blum MT-2B ultramicrotome was used to cut 70–90 nm thin sections. Sections were mounted on 200-mesh copper grids and stained with 2% aqueous uranyl acetate + lead citrate. Sections were examined in a Joel Jem 1400 TEM. An Orius SC1000 bottom-mounted CCD camera was used to capture the images.

Single cell RNASeq analyses

We utilized microfluidic single cell capture and single cell mRNA sequencing technologies to explore genome-wide gene expression in PDAC cells. Fluidigm's C1^{TM} Single-Cell Autoprep System (C1) allows fully automated capture of up to 96 single cells and subsequent cDNA synthesis for the use in QPCR and RNA-sequencing. Initial studies used C1 machines at the University of Pennsylvania and Yale, although our Sequencing Core facility has recently purchased a C1 machine which is currently being used. The cultured MTF cell suspension were loaded into the C1 and by using an integrated fluidic circuit chip, single cells were captured at distinct sites in microfluidic channels. Some heterogeneity in captured cells was evident in the capture sites. After optical confirmation of single cells at each capture site on the chip, the cells were processed for in-line cell lysis, reverse transcription, and cDNA amplification steps. The resultant cDNA was then subjected to Fluidigm's BioMark DELTAgene QPCR assay using a custom-designed 36-marker PDAC panel for this purpose, which included EMT, macrophage, MTF, epithelial, and pancreatic markers (and housekeeping genes). We obtained single cell preparations from 5 patients (and have captured up to 90 single cells, with validated amplifications). Following validation of the QPCR marker panel, we then further utilized the amplified cDNA from each single cell to generate sequencing-ready libraries using Illumina's Nextera XT library preparation kit. The libraries were pooled and sequenced by 1X50bp of total 150 million reads on an Illumina HiSeq 2500, which is sufficient in conducting comprehensive gene expression analysis.

Preprocessing of Illumina reads and transcriptome assembly. The quality of sequence read data for all single cell Illumina libraries was assessed using FastQC (http://www.bioinformatics.babraham.ac.uk/projects/fastqc/; version 0.11.5). Reads were trimmed using Trimmomatic v0.35 [118] with default settings at "ILLUMINACLIP:TruSeq3-SE:2:30:10 LEADING:3 TRAILING:3 SLIDINGWINDOW:4:15 MINLEN:36" to remove Illumina adapter sequences identified by FastQC and low-quality bases. Genome-guided (Ensembl build GRCh38.p7, http://www.ensembl.org/) and de novo assemblies of trimmed reads for all libraries were performed using Trinity r20140717 [119] and TopHat v2.0.14-Cufflinks v2.2.1 [120] respectively. The resulting transcriptome assemblies were each assessed for redundancy using GenomeTools v1.5.4 [121] to remove similar (sub)-sequences, then merged using CD-HIT--EST v4.6 [122]. Only the longest transcripts out of CD-HIT-EST clusters of sequences that shared at least 95% sequence similarity were retained for subsequent downstream analyses.

Expression quantification and quality control. Trimmed reads from each single cell library were mapped against the transcriptome assembly generated from all libraries using the Bowtie2 aligner [123]. The resulting alignment files (BAM files) were then used to estimate the transcript-level abundance by using the RSEM (RNA-Seq by Expectation Maximization) software [124]. TPM (Transcripts Per Million) unit was used as normalized expression values for each library. Expression matrices were created for sample libraries of each patient and combined sample libraries of all patients. Quality control was then performed on the expression

matrices to identify and remove low-quality cells with a mapping rate of less than 50% of sequenced reads [125] and/or half a million total sequenced reads [125–128]. Additionally, transcripts for which more than 25% of cells showed zero expression across all cells [126] and those identified by the functional assignment as either mitochondrially encoded genes (mtDNA) or mitochondrially localized proteins [126, 129] were removed. Suitable samples from 4 patients were included.

Functional assignment. The assembled sequences were compared against 214,837 human cDNAs/non-coding RNA (ncRNA) annotated transcripts from Ensembl build GRCh38.p7 (blastn E-value = 1e-10) and 42,130 human proteins from UniProtKB/SwissProt (blastx E-value = 1e-5). Best scoring blast search targets when were then used to retrieve matching gene description and symbols from both Ensembl Biomart and UniProtKB online databases. KEGG pathway mapping and enrichment analysis of the expressed gene sets in the filtered expression matrices were performed using WebGestalt (WEB-based Gene SeT AnaLysis Toolkit) with the Ensembl human transcripts as reference background [130]. The enrichment analysis was performed using hypergeometric test and p-value (< 0.1) corrected by a Bonferroni multiple testing correction. Pathways selected for enrichment analysis were required to have a minimum of two genes.

Expression clustering. Heatmaps of filtered gene expression matrices were generated with Pheatmap R package version 1.0.8 [131]. Hierarchical clustering analysis was performed based on Euclidean distance to cluster rows (genes), and the cutree algorithm was used to divide rows into gene clusters with similar expression across single cells.

Supporting information

S1 Spreadsheet. Lists of genes contained within Clusters 1, 2, and 3.
(XLSX)

Author Contributions

Conceptualization: Gary A. Clawson.

Data curation: Eric Wafula, Naomi Altman.

Formal analysis: Eric Wafula, Claude dePamphilis, Naomi Altman, Loren Honaas, Thomas Abraham.

Funding acquisition: Gary A. Clawson.

Investigation: Gail L. Matters, Ping Xin, Christopher McGovern, Morgan Meckley, Luke Stewart, Christopher D'Jamoos, Yuka Imamura Kawasawa, Zhen Du.

Methodology: Gary A. Clawson, Gail L. Matters, Claude dePamphilis, Luke Stewart, Christopher D'Jamoos, Naomi Altman, Thomas Abraham.

Project administration: Gary A. Clawson, Gail L. Matters, Joyce Wong.

Resources: Joyce Wong, Luke Stewart, Christopher D'Jamoos, Yuka Imamura Kawasawa, Thomas Abraham.

Software: Eric Wafula, Claude dePamphilis, Naomi Altman, Loren Honaas.

Supervision: Gary A. Clawson, Gail L. Matters.

Validation: Gail L. Matters.

Visualization: Thomas Abraham.

Writing – original draft: Gary A. Clawson.

Writing – review & editing: Gary A. Clawson, Gail L. Matters, Eric Wafula, Joyce Wong, Naomi Altman, Thomas Abraham.

References

1. Rahib L, Smith BD, Aizenberg R, Rosenzweig AB, Fleshman J, Matrisian LM. Projecting cancer incidence and deaths to 2030: the unexpected burden of thyroid, liver, and pancreas cancers in the United States. Cancer Res. 2014; 74(11):2913–21. https://doi.org/10.1158/0008-5472.CAN-14-0155 PMID: 24840647
2. Kulemann B, Pitman MB, Liss AS, Valsangkar N, Fernandes-Del Castillo C, Lillemoe KD, et al. Circulating tumor cells found in patients with localized and advanced pancreatic cancer. Pancreas. 2015; 44(4):547–50. https://doi.org/10.1097/MPA.0000000000000324 PMID: 25822154
3. Ankeny JS, Court CM, Hou S, Li Q, Song M, Wu DC, et al. Circulating tumour cells as a biomarker for diagnosis and staging in pancreatic cancer. Br J Cancer. 2016; 114(12):1367–75. https://doi.org/10.1038/bjc.2016.121 PMID: 27300108
4. Clawson GA. Cancer Metastasis Redux. In: Meyers B, editor. Reviews in Cell Biology and Molecular Medicine: Wiley-VCH; 2015.
5. Chaffer CL, Weinberg D. A perspective on cancer cell metastasis. Science. 2011; 331:1559–64. https://doi.org/10.1126/science.1203543 PMID: 21436443
6. Zhang L, Ridgway LD, Wetzel MD, Ngo J, Yin W, Kumar D, et al. The identifcation and characterization of breast cancer CTCs competent for brain metastasis. Sci Transl Med. 2013; 5(180):ra48.
7. Markiewicz A, Ksiazkiewicz M, Seroczynska B, Skokowski J, Szade J, Welnicka-Jaskiewicz M, et al. Heterogeneity of mesenchymal markers expression-molecular profiles of cancer cells disseminated by lymphatic and hematogenous routes in breast cancer. Cancers (Basel). 2013; 5(4):1485–503.
8. Li YM, Xu SC, Li J, Han KQ, Pi HF, Zheng L, et al. Epithelial-mesenchymal transition markers expressed in circulating tumor cells in hepatocellular carcinoma patients with different stages of disease. Cell Death Dis. 2013; 4:e831. https://doi.org/10.1038/cddis.2013.347 PMID: 24091674
9. Friedlander TW, Ngo VT, Dong H, Premasekharan G, Weinberg V, Doty S, et al. Detection and characterization of invasive circulating tumor cells derived from men with metastatic castration-resistant prostate cancer. Int J Cancer. 2014; 134(10):2284–93. https://doi.org/10.1002/ijc.28561 PMID: 24166007
10. Friedlander TW, Premasekharan G, Paris PL. Looking back, to the future of circulating tumor cells. Pharmacol Ther. 2013;S0163–7258.
11. Baccelli I, Schneeweiss A, Riethdorf S, Stenzinger A, Schillert A, Vogel V, et al. Identification of a population of blood circulating tumor cells from breast cancer patients that initiates metastsis in a xenograft assay. Nat Biotech. 2013; 31:539–44.
12. Grover PK, Cummins AG, Price TJ, Roberts-Thomson IC, Hardingham JE. Circulating tumour cells: the evolving concept and the inadequacy of their enrichment by EpCAM-based methodology for basic and clinical cancer research. Ann Oncol. 2014;March 20 Epub.
13. Cristofanilli M, Budd G, Ellis M, Stopeck A, Matera J, Miller M, et al. Circulating tumor cells, disease progression, and survival in metastatic breast cancer. N Engl J Med. 2004; 351(8):824–6.
14. Cohen SJ, Punt CJ, Iannotti N, Saidman BH, Sabbath KD, Gabrail NY, et al. Relationship of circulating tumor cells to tumor response, progression-free survival, and overall survival in patients with metastatic colorectal cancer. J Clin Oncol. 2008; 26:3213–21. https://doi.org/10.1200/JCO.2007.15.8923 PMID: 18591556
15. Ma X, Xiao Z, Li X, Wang F, Zhang J, Zhou R, et al. Prognostic role of circulating tumor cells and disseminated tumor cells in patients with prostate cancer: a systematic review and meta-analysis. Tumour Biol. 2014;Feb22 Epub.
16. Karamitopoulou E, Zilobec I, Born D, Kondi-Pafiti A, Lykoudis P, Mellou A, et al. Tumor budding is a strong and independent prognostic factor in pancreatic cancer. Eur J Cancer. 2013; 49:1032–9. https://doi.org/10.1016/j.ejca.2012.10.022 PMID: 23177090
17. Karamitopoulou E. Tumor budding cells, cancer stem cells and epithelial-mesenchymal transition-type cells in pancreatic cancer. Front Oncology. 2013; 2:209.
18. Clawson GA. Cancer. Fusion for moving. Science. 2013; 342(6159):699–700. https://doi.org/10.1126/science.1244270 PMID: 24202164
19. Pawelek JM, Chakraborty AK. The cancer cell-leukocyte fusion theory of metastasis. Adv Cancer Res. 2008; 101:397–444. https://doi.org/10.1016/S0065-230X(08)00410-7 PMID: 19055949

20. Lazova R, LeBerge GS, Duvall E, Spoelstra N, Klump V, Sznol M, et al. A melanoma brain metastasis with a donor-patient hybrid genome following bone marrow transplantation: first evidence for fusion in human cancer. PLoS One. 2013; 8(6):e66731. https://doi.org/10.1371/journal.pone.0066731 PMID: 23840523

21. Dittmar T, Nagler C, Niggemann B, Zanker KS. The dark side of stem cells:; triggering cancer progression by cell fusion. Curr Mol Med. 2013; 13(5):357–50.

22. Duelli D, Lazebnik Y. Cell fusion: a hidden enemy? Cancer Cell. 2003; 3:445–8. PMID: 12781362

23. Powell AE, Anderson EC, Davies PS, Silk AD, Pelz C, Impey S, et al. Fusion between intestinal epithelial cells and macrophages in a cancer context results in nuclear reprogramming. Cancer Res. 2011; 71:1497–505. https://doi.org/10.1158/0008-5472.CAN-10-3223 PMID: 21303980

24. Clawson GA, Matters GL, X P., Imamura-Kawasawa Y, Du Z, Thiboutot DM, et al. Macrophage-tumor cell fusions from peripheral blood of melanoma patients. PLoS ONE. 2015;Accepted. https://doi.org/10.1371/journal.pone.0134320

25. Ren D, Li H, Sun J, Guo P, Han H, Yang Y, et al. Novel insight into MALAT-1 in cancer: Therapeutic targets and clinical applications. Oncol Lett. 2016; 11(3):1621–30. https://doi.org/10.3892/ol.2016.4138 PMID: 26998053

26. Liu JH, Chen G, Dang YW, Luo DZ. Expression and prognostic significance of lncRNA MAALAT1 in pancreatic cancer tissues. Asian Pac J Cancer Prev. 2014; 15(7):2971–7. PMID: 24815433

27. Funamizu N, Hu C, Lacy C, Schetter A, Zhang G, He P, et al. Macrophage migration inhbitory factor induces epithelial to mesenchymal transition, enhances tumor aggressiveness and predicts clinical outcome in resected pancreatic ductal adenocarcinoma. Int J Cancer. 2013;Epub Jul 23.

28. Zhang L, Ye SB, Ma G, Tang XF, Chen SP, He J, et al. Th expressions of MIF and CXCR4 protein in tumor microenvironment are adverse prognostic factors in patients with esophageal squamous cell carcinoma. J Transl Med. 2013; 11 (Mar 8):60.

29. Krieg A, Riemer JC, Telan LA, Gabbert HE, Knoefel T. CXCR4—A prognostic and clinicopathological biomarker for pancreatic ductal adenocarcinoma: A meta-analysis. PLoS One. 2015; 10(6):e0130192. https://doi.org/10.1371/journal.pone.0130192 PMID: 26091099

30. Guo D, Duo J, Yao J, Jiang K, Hu J, Wang B, et al. D-dopachrome tautomerase is over-expressed in pancreatic ductal adenocarcinoma and acts cooperatively with macrophage migration inhibitory faqctor to promote cancer growth. Int J Cancer. 2016; 139(9):2056–67. https://doi.org/10.1002/ijc.30278 PMID: 27434219

31. Costa-Silva B, Aiello NM, Ocean AJ, Singh S, Zhang H, Thakur BK, et al. Pancreatic cancer exosomes initiate pre-metastatic niche formation in the liver. Nat Cell Biol. 2015; 17(6):816–26. https://doi.org/10.1038/ncb3169 PMID: 25985394

32. Lo MC, Yip TC, Ngan KC, Cheng WW, Law CK, Chan PS, et al. Role of MIF/CXCL8/CXCR2 signaling in the growth of nasopharyngeal carcinoma tumor spheres. Cancer Lett. 2013;Epub Feb 8.

33. Bernhagen J, Krohn R, KLue H, Gregory JL, Zernecke A, Koenen RR, et al. MIF is a noncognate ligand of CXC chemokine receptors in inflammatory and atherogenic cell recruitment. Nat Med. 2007; 13:587–96. https://doi.org/10.1038/nm1567 PMID: 17435771

34. Shi X, Leng L, Wang T, Wang W, Du X, Li J, et al. CD44 is the signaling component of the macrophage migration inhibitory factor-CD74 receptor complex. Immunity. 2006; 25:595–606. https://doi.org/10.1016/j.immuni.2006.08.020 PMID: 17045821

35. Brown KE, Bagci H, Soza-Ried J, Fisher AG. Atypical heterochromatin organization and replication are rapidly acquired by somatic cells following fusion-mediated reprogramming by mouse ESCs. Cell Cycle. 2013; 12:3253–61. https://doi.org/10.4161/cc.26223 PMID: 24036550

36. Huisman A, Ploeger LS, Dullens H, Jonges TN, Belien JA, Meijer GA, et al. Discrimination between benign and malignant prostate tissue using chromatin texture analysis in 3-D by confocal laser scanning microscopy. The Prostate. 2006; 67:248–54.

37. Pizarro JG, Cristofari G. Post-transcriptional control of LINE-1 retrotransposition by cellular host factors in somatic cells. Front Cell Dev Biol. 2016; 4:14. https://doi.org/10.3389/fcell.2016.00014 PMID: 27014690

38. Wu T, Li Y, Liu B, Zhang S, Wu L, Zhu X, et al. Expression of Ferritin Light Chain (FTL) is elevated in glioblastoma and FTL silencing inhibits glioblastoma cell proliferation via the GADD45/JNK pathway. PLoS One. 2016; 11(2):e0149361. https://doi.org/10.1371/journal.pone.0149361 PMID: 26871431

39. Chekhun SV, Lukyanova NY, Shvets YV, Burlaka AP, Buchinska LG. Signifiance of ferritin expression in formation of malignant phenotype of human breast cancer cells. Exp Oncol. 2014; 36(3):179–83. PMID: 25265351

40. Jezequel P, Champion L, Spyratos F, Loussouarn D, Campone M, Guerin-Charbonnel C, et al. Validation of tumor-associated macrophage ferritin light chain as a prognostic biomarker in node-negative

breast cancer tumors: A multicentric 2004 national PHRC study. Int J Cancer. 2012; 131(2):426–37. https://doi.org/10.1002/ijc.26397 PMID: 21898387

41. Marimastat: BB2516, TA2516. Drugs Res Dev. 2003; 4:198–203.
42. Wang G, GRier DD, Woo J, Ward M, Sui G, Torti SV, et al. Ferritin H is a novel m arker of early erythroid precursors and macrophages. Histopathology. 2013; 62(6):931–40. https://doi.org/10.1111/his.12101 PMID: 23611361
43. Tang X. Tumor-associated macrophages as potential diagnostic and prognostic biomarkers in breast cancer. Cancer Lett. 2013; 332(1):3–10. https://doi.org/10.1016/j.canlet.2013.01.024 PMID: 23348699
44. Hou YC, Chao YJ, Tung HL, Wang HC, Shan YS. Coexpression of CD-44-positive/CD133-positive cancer stem cells and CD204-positive tumor-associated macorphages is a predictor of survival in pancreatic ductal adenocarcinoma. Cancer. 2014; 120(17):2766–77. https://doi.org/10.1002/cncr.28774 PMID: 24839953
45. Sevenich L, Bowman RL, Mason SD, Quail DF, Rapaport F, Elie BT, et al. Analysis fo tumour- and stroma-supplied proteolytic networks reveals a brain-metastasis-promoting role for cathepsin S. Nat Cell Biol. 2014; 16(9):878–88.
46. Gemoli T, Epping F, Heinrich L, Fritzche B, Roblick UJ, Szymczak S, et al. Increased cathepsin D protein expression is a biomarker for oxsteosarcomas, pulmonary metastases and other bone malignancies. Oncotarget. 2015; 6(18):16517–26. https://doi.org/10.18632/oncotarget.4140 PMID: 26203049
47. Yang WE, Ho CC, Yang SF, Lin SH, Yeh KT, Lin CW, et al. Cathepsin B expression and the correlation with clinnical aspects of oral squamouns cell carcinoma. PLoS One. 2016; 11(3):e0152165. https://doi.org/10.1371/journal.pone.0152165 PMID: 27031837
48. Ruan J, Zheng H, Rong X, Zhang J, Fang W, Zhao P, et al. Over-expression of cathepsin B in hepatocellular carcinomas predicts poor prognosis of HCC patients. Mol Cancer. 2016; 15:17. https://doi.org/10.1186/s12943-016-0503-9 PMID: 26896959
49. Cano CE, Sandi MJ, Hamidi T, CAlvo EL, Turrini O, Bartholin L, et al. Homotypic cell cannibalism, a cell-death process regulated by the nuclear protein 1, opposes to metastasis in pancreatic cancer. EMBO Mol Med. 2012; 4(9):964–79. https://doi.org/10.1002/emmm.201201255 PMID: 22821859
50. Du P, Ye L, Yang Y, Jiang WG. Candidate of metastasis 1 regulates in vitro growth and invasion of bladder cancer cells. Int J Oncol. 2013; 42(4):1249–56. https://doi.org/10.3892/ijo.2013.1802 PMID: 23443904
51. Lee YK, Jee BA, Kwon SM, Yoon YS, Xu WG, Wang HJ, et al. Identifcation of a mitochondrial defect gene signature reveals NUPR1 as a key regulator of liver cancer progression. Hepatology. 2015; 62(4):1174–89. https://doi.org/10.1002/hep.27976 PMID: 26173068
52. Guo X, Wang W, Hu J, Feng K, Pan Y, Zhang L, et al. Lentivirus-mediated RNAi knockdown of NUPR1 inhibits human nonsmall cell lung cancer growth in vitro and in vivo. Anat Rec(Hoboken). 2012; 295(12):2114–21.
53. Li Y, Li Y, Chen W, He F, Tan Z, Zheng J, et al. NEAST expression is associated with tumor recurrence and unfavorable prognosis in colorectal cancer. Oncotarget. 2015; 6(29):27641–50. https://doi.org/10.18632/oncotarget.4737 PMID: 26314847
54. Guo S, Chen W, Luo Y, Ren F, Zhong T, Rong M, et al. Clinical implication of long non-coding RNA NEAT1 expression in hepatocellular carcinoma patients. Int J Cliin Exp Pathol. 2015; 8(5):5395–402.
55. Zhang XD, Qi L, Wu JC, Qin ZH. DRAM1 regulates autophagy fllux through lysosomes. PLoS One. 2013; 8(5):e63245. https://doi.org/10.1371/journal.pone.0063245 PMID: 23696801
56. Liu J, Peng WX, Mo YY, Luo D. MALAT1-mediated tumorigenesis. Front Biosci(Landmark Ed). 2017; 22:66–80.
57. Wei Y, Niu B. Role of MALAT1 as a prognostic factor for survival in various caners: A systematic review of the literature with meta-analysis. Dis Markers. 2015; 2015(ID#164635).
58. Gustschner T, Hammerle M, Eissmann M, Hsu J, Kim Y, Hung G, et al. The noncoding RNA MALAT1 is a critical regulator of the metastasis phenotype in lung cancer cells. Cancer Res. 2013; 73(3):1180–9. https://doi.org/10.1158/0008-5472.CAN-12-2850 PMID: 23243023
59. Jiao F, Hu H, Yuan C, Wang L, Jiang WG, Jin Z, et al. Elevated expression level of long noncoding RNA MALAT-1 facilitates cell growth, migration and invasion in pancreatic cancer. Oncol Rep. 2014; 32(6):2485–92. https://doi.org/10.3892/or.2014.3518 PMID: 25269958
60. Kanno H, Nishihara H, Wang L, Yuzawa S, Kobayashi H, Tsuda M, et al. Expression of CD163 prevents apoptosis through the production of granulocyte colony-stimulating factor in meningioma. Neuro Oncol. 2013; 17(7):853–64.

61. Lan C, Huang X, Lin S, Huang H, Cal Q, Wan T, et al. Expression of M2-polarized macrophages is associated with poor prognosis for advanced epithelial ovarian cancer. Technol Cancer Res Treat. 2013; 12(3):259–67. https://doi.org/10.7785/tcrt.2012.500312 PMID: 23289476

62. Matsumura Y, Ishii G, Aokage K, Kuwata T, Hishida T, Yoshida J, et al. Morphophenotypic characteristics of intralymphatic cancer and stromal cells susceptible to lymphogenic metastasis. Cancer Sci. 2012; 103(7):1342–7. https://doi.org/10.1111/j.1349-7006.2012.02275.x PMID: 22429811

63. Salmi M, Karikoski M, Elima K, Rantakari P, Jalkanen S. CD44 binds to macrophage mannose receptor on lymphatic endothelium and supports lymphocyte migration via afferent lymphatics. Circ Res. 2013; 112(12):1577–82. https://doi.org/10.1161/CIRCRESAHA.111.300476 PMID: 23603511

64. Swierczynski J, Hebanowska A, Sledzinski T. Role of abnormal lipid metabolism in development, progression, diagnosis and therapy of pancreatic cancer. World J Gastroenterol. 2014; 20(9):2279–303. https://doi.org/10.3748/wjg.v20.i9.2279 PMID: 24605027

65. Baenke F, Peck B, Miess H, Schulze A. Hooked on fat: the role of lipid synthesis in cancer metabolism and tumour development. Dis Model Mech. 2013; 6(6):1353–63. https://doi.org/10.1242/dmm.011338 PMID: 24203995

66. Seguin F, Carvalho MA, Bastos DC, Agostini M, Zecchin KG, Alvarez-Flores MP, et al. The fatty acid synthase inhibitor orlistat reduces experimental metastases and angiogenesis in B16-10 melanomas. Br J Cancer. 2012; 107(6):077–87.

67. Zecchin KG, Rossato FA, Raposo HF, Melo DR, Alberici LC, Oliveira HC, et al. Inhibition of faqtty acid synthase in melanoma cells activates the intrinsic pathway of apoptosis. Lab Invest. 2011; 91(2):232–40. https://doi.org/10.1038/labinvest.2010.157 PMID: 20805790

68. de Andrade BA, Leon JE, Carlos R, Delgado-Azanero W, Mosqueda-Taylor A, Graner E, et al. Expression of fatty acid synthase (FASN) in oral nevi and melanoma. Oral Dis. 2011; 17(8):808–12. https://doi.org/10.1111/j.1601-0825.2011.01841.x PMID: 21819495

69. Pandev V, Vijayakumar MV, Ajay AK, Malvi P, Bhat MK. Diet-induced obesity increases melanoma progression: involvement of Cav-1 and FASN. Int J Cancer. 2012; 130(2):497–508.

70. Madsen DH, Leonard D, Masedunskas A, Moyer A, Jurgensen HJ, Peters DE, et al. M2-like macrophages are responsible for collagen degradation through a mannose receptor-mediated pathway. J Cell Biol. 2013; 202:951–66. https://doi.org/10.1083/jcb.201301081 PMID: 24019537

71. Galdiero MR, Garlanda C, Jaillon S, Marone G, Mantovani A. Tumor associated macrophages and neutrophils in tumor progression. J Cell Physiol. 2013; 228(7):1404–12. https://doi.org/10.1002/jcp.24260 PMID: 23065796

72. Sica A, Larghi P, Mancino A, Rubino L, Porta C, Totaro MG, et al. Macrophage polarization in tumour progression. Semin Cancer Biol. 2008; 18:349–55. https://doi.org/10.1016/j.semcancer.2008.03.004 PMID: 18467122

73. Kurahara H, Shinchi H, Mataki Y, Maemura K, Noma H, Kubo F, et al. Significance of M2-polarized tumor-associated macrophage in pancreatic cancer. J Surg Res. 2011; 167:e211–9. https://doi.org/10.1016/j.jss.2009.05.026 PMID: 19765725

74. Laoui D, Van Overmeire E, Di Conza G, Aldeni C, Keirsse J, Morias Y, et al. Tumor hypoxia does not drive differentiation of tumor-associated macrophages but rather fine-tunes the M2-like macrophage population. Cancer Res. 2013;Epub Nov 12.

75. Liu CY, Xu JY, Shi XY, Huang W, Ruan TY, Xie P, et al. M2-polarized tumor-associated macrophages promoted epithelial-mesenchymal transition in pancreatic cancer cells, partially through TLR4/IL-10 signaling pathway. Lab Invest. 2013; 93(7):844–54. https://doi.org/10.1038/labinvest.2013.69 PMID: 23752129

76. Bonde AK, Tsischler V, Kumar S, Soltermann A, Schwendener RA. Intratumoral macrophages contribute to epithelial-mesenchymal transition in solid tumors. BMC Cancer. 2012; 12:35. https://doi.org/10.1186/1471-2407-12-35 PMID: 22273460

77. Shabo I, Olsson H, Sun XE, Svanvik J. Expression of the macrophage antigen CD163 in rectal cancer cells is associated with early local recurrence and reduced survival time. Int J Cancer. 2009; 125:1826–31. https://doi.org/10.1002/ijc.24506 PMID: 19582880

78. Shabo I, Stal O, Olsson H, Dore S, Svanvik J. Breast cancer expression of CD163, a macrophage scavenger receptor, is related to early distant recurrence and reduced patient survival. Int J Cancer. 2008; 123(4):780–6. https://doi.org/10.1002/ijc.23527 PMID: 18506688

79. Shabo I, Svanvik J. Expression of macrophage antigens by tumor cells. Adv Exp Med Biol. 2011; 714:141–50. https://doi.org/10.1007/978-94-007-0782-5_7 PMID: 21506012

80. Ding J, Jin W, Chen C, Shao Z, Wu J. Tumor associated macrphage X cancer cell hybrids may acquire cancer stem cell properties in breast cancer. PLoS One. 2012; 7:e41942. https://doi.org/10.1371/journal.pone.0041942 PMID: 22848668

81. Meyer-Siegler KL, Vera PL, Iczkowski KA, Bifulco C, Lee A, Gregersen PK, et al. Macrophage migration inhibitory factor (MIF) gene polymorphisms are associated with increased prostate cancer incidence. Genes Immun. 2007; 8:646–52. https://doi.org/10.1038/sj.gene.6364427 PMID: 17728788

82. Kindt N, Lechien J, Decaestecker C, Rodriguez A, Chantrain G, Remmelink M, et al. Expression of macrophage migration-inhibitory factor is correlated with progression in oral cavity carcinomas. Anticancer Res. 2012; 32(10):4499–505. PMID: 23060578

83. Schulz R, Marchenko ND, Holembowski L, Fingerle-Rowson G, Pesic M, Zender L, et al. Inhibiting the HSP90 chaperone destabilizes macrophage migration inhibitory factor and thereby inhibits breast tumor progression. J Exp Med. 2012; 209(2):275–89. https://doi.org/10.1084/jem.20111117 PMID: 22271573

84. Wilson JM, Coletta PL, Cuthbert RJ, Scott N, MacLennan K, Hawcroft G, et al. Macrophage migration inhibitory factor promotes intestinal tumorigenesis. Gastroenterology. 2005; 129:1485–503. https://doi.org/10.1053/j.gastro.2005.07.061 PMID: 16285950

85. Wang D, Luo L, Chen W, Chen LZ, Zeng WT, Li W, et al. Significance of the vascular endothelial growth factor and the macrophage migration inhibitory factor in the progression of hepatocellular carcinoma. Oncol Rep. 2014; 31(3):1199–204. https://doi.org/10.3892/or.2013.2946 PMID: 24366206

86. Schulz R, Moll UM. Targeting the heat shock protein 90: a rational way to inhibit macrophage migration inhibitory factor function in cancer. Curr Opin Oncol. 2014; 26(1):108–13. https://doi.org/10.1097/CCO.0000000000000036 PMID: 24225413

87. Verschuren L, Kooistra T, Bernhagen J, Voshol PJ, Ouwens DM, van Erk M, et al. MIF deficiency reduces chronic inflammation in white adipose tissue and impairs the development of insulin resistance, glucose intolerance, and associated atherosclerotic disease. Circ Res. 2009; 105:99–107. https://doi.org/10.1161/CIRCRESAHA.109.199166 PMID: 19478200

88. Yaddanapudi K, Putty K, Rendon BE, Lamont GJ, Faughn JD, Satoskar A, et al. Control of tumor-associated macrophage alternative activation by macrophage migration inhibitory factor. J Immunol. 2013; 190(6):2984–93. https://doi.org/10.4049/jimmunol.1201650 PMID: 23390297

89. Liu C-Y, Xu J-Y, Shi X-Y, Huang W, Ruan T-Y, Xie P, et al. M2-polarized tumor-associated macrophages promoted epithelial-mesenchymal transition in pnacratic cancer cells, partially through TLR4-IL-10 signaling pathway. Lab Invest. 2013; 93:844–54. https://doi.org/10.1038/labinvest.2013.69 PMID: 23752129

90. Yoshikawa K, Mitsunaga S, Kinoshita T, Konishi M, Takahashi S, Gotohda N, et al. Impact of tumor-associated macrophages on invasive ductal carcinoma of the pancreas head. Cancer Sci. 2012; 103 (11):2012–20. https://doi.org/10.1111/j.1349-7006.2012.02411.x PMID: 22931216

91. Mitchem JB, Brennan DJ, Knolhoff BL, Belt BA, Zhu Y, Sanford DE, et al. Targeting tumor-infiltrating macrophages decreases tumor-initiating cells, relieves immunosuppression, and improves chemotherapeutic responses. Cancer Res. 2013; 73(31128–41.).

92. Koong AC, Denko NC, Hudson KM, Schindler C, Swiersz L, Koch C, et al. Candidate genes for the hypoxic tumor phenotype. Cancer Res. 2000; 60:883–7. PMID: 10706099

93. Baugh J, Gantier M, Li L, Byrne A, BUckley A, Donnelly SC. Dual regulation of macrophage migration inhibitory factor (MIF) expression in hypoxa by CREB and HIF-1. Biochem Biophys Res Commun. 2006; 347:895–903. https://doi.org/10.1016/j.bbrc.2006.06.148 PMID: 16854377

94. Cui Y, Zhang D, Jia Q, Li T, Zhang W, Han J. Proteomic and tissue array profiling identifies elevated hypoxia-regulated proteins in pancreatic ductal adenocarcinoma. Cancer Invest. 2009; 27:747–55. https://doi.org/10.1080/07357900802672746 PMID: 19488907

95. Winner M, Koong AC, Rendon BE, Zundel W, Mitchell RA. Amplification of tumor hypoxic responses by macrophage migration inhibitory factor-dependent hypoxia-inducible factor stabilization. Cancer Res. 2007; 67:186–93. https://doi.org/10.1158/0008-5472.CAN-06-3292 PMID: 17210698

96. Kyriakis JM. Thinking outside the box about Ras. J Biol Chem. 2009; 284:10993–4. https://doi.org/10.1074/jbc.R800085200 PMID: 19091742

97. Denz A, Pilarsky C, Muth D, Ruckert F, Saeger HD, Grutzmann R. Inhibition of MIF leads to cell cycle arrest and apoptosis in pancreatic cancer cells. J Surg Res. 2010; 160:29–34. https://doi.org/10.1016/j.jss.2009.03.048 PMID: 19726058

98. Long J, Luo GH, Liu C, Cui X, Satoh K, Xiao Z, et al. Development of a unique mouse model for pancreatic cancer lymphatic metastasis. Int J Oncol. 2012; 41(5):1662–8. https://doi.org/10.3892/ijo.2012.1613 PMID: 22941445

99. Harouaka R, Kang Z, Zheng SY, Cao L. Circulating tumor cells: advances in isolation and analysis, and challenges for clinical applications. Pharmacol Ther. 2014; 141:209–21. https://doi.org/10.1016/j.pharmthera.2013.10.004 PMID: 24134902

100. Ting DT, Wittner BS, Ligorio M, Jordan NV, Shah AM, Miyamoto DT, et al. Single-Cell RNA sequencing identifies extracellular matrix gene expression by pancreatic circulating tumor cells. Cell Reports. 2014; 8:1905–18. https://doi.org/10.1016/j.celrep.2014.08.029 PMID: 25242334

101. Rhim A, Mirek E, Aiello N, al. e. EMT and dissemination precede pancreatic tumor formation. Cell. 2012; 148:349–61. https://doi.org/10.1016/j.cell.2011.11.025 PMID: 22265420

102. Rhim A, al. e. Detection of circulating pancreas epithelial cells in patients with pancreatic cystic lesions. Gastroenterology. 2014; 146:647–51. https://doi.org/10.1053/j.gastro.2013.12.007 PMID: 24333829

103. Kamphues C, Al-Abadi H, Durr A, Al-Abadi N, Schricke D, Bova R, et al. DNA index as a strong prognostic factor in patients with adenocarcinoma of the pancreatic head: results of a 5-year prospective study. Pancreas. 2013; 42(5):807–12. https://doi.org/10.1097/MPA.0b013e3182773eb6 PMID: 23271398

104. Eskelinen M, Lipponen P, Marin S, Haapasalo H, Makinen K, Puittinen J, et al. DNA ploidy, S-phase fraction, and G2 fraction as prognostic determinants in human pancreatic cancer. Scand J Gastroenterol. 1992; 27(1):39–43. PMID: 1736340

105. Eskelinen M, Lipponen P, Collan Y, Marin S, Alhava E, Nordling S. Relationship between DNA ploidy and survival in patients with exocrine pancreatic cancer. Pancreas. 1991; 6:90–5. PMID: 1994384

106. Tsavaris N, Kavantzas N, Tsigritis K, Xynos ID, Papadoniou N, Lazaris A, et al. Evaluation of DNA ploidy in relation with established prognostic factors in patients with locally advanced (unresectable) or metastatic pancreatic adenocarcinoma: a retrospective analysis. BMC Cancer. 2009; 9:264. https://doi.org/10.1186/1471-2407-9-264 PMID: 19646258

107. Xynos ID, Kavantzas N, Tsaousi S, Zacharakis M, Agrogiannis G, Kosmas C, et al. Factors influencing survival in Stage IV colorectal cancer: the influence of DNA ploidy. ISRN Gastroenterol. 2013; 2013:490578. https://doi.org/10.1155/2013/490578 PMID: 23840958

108. Lazebnik Y. The shock of being united and symphiliosis. Another lesson from plants? Cell Cycle. 2014; 13: 2323–29. https://doi.org/10.4161/cc.29704 PMID: 25483182

109. Goldenberg DM, Rooney RJ, Loo M, Liu DP, Chang C-H. In-Vivo fusion of human cancer and hamster stromal cells permanently transduces and transcribes human DNA. PLoS One. 2014; 9(9):e107927. https://doi.org/10.1371/journal.pone.0107927 PMID: 25259521

110. Mijaljica D, Devenish RJ. Nucleophagy at a glance. J Cell Sci. 2013; 126:4325–30. https://doi.org/10.1242/jcs.133090 PMID: 24013549

111. Fenech M, Kirsch-Volders M, Natarajan AT, Surralles J, Crott JW, Parry J, et al. Molecular mechanisms of micronucleus, nucleoplasmic bridge and nuclear bud formation in mammalian and human cells. Mutagenesis. 2011; 26:125–32. https://doi.org/10.1093/mutage/geq052 PMID: 21164193

112. Rello-Varona S, Lissa D, Shen S, Niso-Santano M, Senovilla L, Marino G, et al. Autophagic removal of micronuclei. Cell Cycle. 2012; 11:170–7. https://doi.org/10.4161/cc.11.1.18564 PMID: 22185757

113. Park YE, Hayashi YK, Bonne G, Arimura T, Noguchi S, Nonaka I, et al. Autophagic degradation of nuclear components in mammalian cells. Autophagy. 2009; 5:795–804. PMID: 19550147

114. Pathania AS, Wani ZA, Guru SK, Kumar S, Bhushan S, Korkaya H, et al. The anti-angiogenic and cytotoxic effects of the boswellic acid analog BA145 are potentiated by autphagy inhibitors. Mol Cancer. 2015; 14:6. https://doi.org/10.1186/1476-4598-14-6 PMID: 25608686

115. Pedersen IM, Zisoulis DG. Transposable elements and miRNA: Regulation of genomic stability and plasticity. Mob Genet Elements. 2016; 6(3):e1175537. https://doi.org/10.1080/2159256X.2016.1175537 PMID: 27511122

116. Rangasamy D, Lenka N, Ohms S, Dahlstrom JE, Blackburn AC, Board PG. Activation of LINE-1 retrotransposon increases the risk of epithelial-mesenchymal transition and metastasis in epithelial cancer. Curr Mol Med. 2015; 15(7):588–97. https://doi.org/10.2174/1566524015666150831130827 PMID: 26321759

117. Clawson GA, Kimchi E, Patrick SD, Xin P, Harouaka R, Zheng S, et al. Circulating tumor cells in melanoma patients. PLoS One. 2012; 7(7):e41052. https://doi.org/10.1371/journal.pone.0041052 PMID: 22829910

118. Bolger AM, Lohse M, Usadel B. "Trimmomatic: a flexible trimmer for Illumina sequence data". Bioinformatics. 2014;btu170.

119. Grabherr MG, Haas BJ, Yassour M, Levin JZ, Thompson DA, Amit I, et al. Full-length transcrriptome assembly from RNA-Seq data without a reference genome. Nature Biotech. 2011; 29(7):644–52.

120. Trapnell C, Roberts AB, Goff L, Pertea G, Kim D, Kelley DR, et al. Differential gene and transcript expression analysis of RNA-seq experiments with TopHat and Cufflinks. Nature Protocols. 2012; 7(3):562–78. https://doi.org/10.1038/nprot.2012.016 PMID: 22383036

121. Gordon G, Steinbiss S, Kurtz S. GenomeTools: a comprehensive software library for efficient processing of structured genome annotations. IEEE/ACM Transactions on Computational Biol Informatics. 2013; 10(2):645–56.

122. Li W, Godzik A. Cd-hit: a fast program for clustering and comparing large sets of protein or nucleotide sequences. Bioinformatics. 2006; 22(13):1658–9. https://doi.org/10.1093/bioinformatics/btl158 PMID: 16731699

123. Langmead B, Salzberg SL. Fast gapped-read alignment with Bowtie 2. Nature Methods. 2012; 9 (4):357–9. https://doi.org/10.1038/nmeth.1923 PMID: 22388286

124. Li B, Dewey CN. RSEM: accurate transcript quantification from RNA-Seq data with or without a reference genome. BMC Informatics. 2011; 12(1):1.

125. Stegle O, Teichmann SA, Marioni JC. Computational and analytical challenges i single-cell transcriptomics. Nature Rev Genetics. 2015; 16(3):133–45.

126. Bacher R, Kendziorski C. Design and computational analysis of single-cell RNA-sequencing experiments. Genome Biol. 2016; 17(1):1.

127. Pollen AA, Nowakowski TJ, Shuga J, Wang X, Leyrat AA, Lui JH, et al. Low-coverage single-cell mRNA sequencing reveals cellular heterogeneity and activated signaling pathways in developing cerebral cortex. Nature Biotech. 2014; 32(10):1053–8.

128. Wu AR, Neff NF, Kalisky T, Dalerba P, Treutlein B, Rothenberg ME, et al. Quantitative assessment of single-cell RNA-sequencing methods. Nature Methods. 2014; 11(1):41–6. https://doi.org/10.1038/nmeth.2694 PMID: 24141493

129. Ilicic T, Kim JK, Kolodziejczyk AA, Bagger FO, McCarthy DJ, Marioni JC, et al. Classification of low wuality cells from single-cell RNA-seq data. Genome Biol. 2016; 17:29. https://doi.org/10.1186/s13059-016-0888-1 PMID: 26887813

130. Wang J, al. e. WEB-based gene set analysis toolkit (Webgestalt): update 2013. Nucl Acid Res. 2013; 41(W1):W77–W83.

131. Kolde R. Pheatmap: pretty heatmaps. R package version 61. 2012.

132. Ke Q, Wu J, Ming B, Zhu S, Yu M, Wang Y, et al. Identification of the PAG1 gene as a novel target of inherent radioresistance inhuman laryngeal carcinoma cells. Cancer Biother Radiopharm. 2012; 27 (10):678–84. https://doi.org/10.1089/cbr.2012.1191 PMID: 22994656

133. Zhou D, Dong P, Li YM, Guo FC, Zhang AP, Song RZ, et al. Overexpression of Csk-binding protein decreases growth, invasion, and migration of esophageal carcinoma cells by controlling Src activation. World J Gastroenterol. 2015; 21(6):1814–20. https://doi.org/10.3748/wjg.v21.i6.1814 PMID: 25684946

134. Ikuta S, Itoh F, Hinoda Y, Toyota M, Malkiguchi Y, Imai K, et al. expression of cytoskeletal-associated protein tyrosine phosphatase PTPH1 imRNA in human hepatocellular carcinoma. J Gastroenterol. 1994; 29(6):727–32. PMID: 7874267

135. Gawlik-Rzemieniewska N, Bednarek I. The role of NANOG transcriptional factor in the development of malignant phenotype of cancer cells. Cancer Biol Ther. 2016; 17(1):1–10. https://doi.org/10.1080/15384047.2015.1121348 PMID: 26618281

136. Wang H, Jiang SW, Zhang Y, Pan K, Xia J, Chen M. High expression of thymosin beta 10 predicts poor prognosis for hepatocellular carcinoma after hepatectomy. World J Surg Oncol. 2014; 12:226. https://doi.org/10.1186/1477-7819-12-226 PMID: 25037578

137. Zhang XJ, Su YR, Liu DJ, Xu DB, Zeng MS, Chen WK. Thymosin beta 10 correlates with lymph node metastases of papillary thyroid carcinoma. J Surg Res. 2014; 192(2):487–93. https://doi.org/10.1016/j.jss.2014.05.066 PMID: 24974154

138. Lee SM, Na YK, Hong H,.S., Jang EJ, Yoon GS, Park JY, et al. Hypomethylation of the thymosin beta (10) gene is not associated with its overexpression in non0small cell lung cancer. Mol Cells. 2011; 32 (4):343–8. https://doi.org/10.1007/s10059-011-0073-z PMID: 22038593

139. Capello M, Ferri-Borgogno S, Riganti C, Chattaragada MS, Principe ML, Roux C, et al. Targeting the Warburg effect in cancer cells through ENO1 knockdown rescues oxidative phosphorylation andinduces growth arrest. Oncotarget. 2016; 7(5):5598–612. https://doi.org/10.18632/oncotarget.6798 PMID: 26734996

140. Principe ML, Ceruti P, Shih NY, Chattaragada MS, Rolla S, Conti L, et al. Targeting of surface alpha-enolase inhibits the invasiveness of pancreatic cancer cells. Oncotarget. 2015; 6(13):11098–113. https://doi.org/10.18632/oncotarget.3572 PMID: 25860938

141. Zhao M, Fang W, Wang Y, Guo S, Shu L, Wang L, et al. Enolase-1 is a therapeutic target in endometrial carcinoma. Oncotarget. 2015; 6(17):15610–27. https://doi.org/10.18632/oncotarget.3639 PMID: 25951350

142. Torres C, Linares A, Alejandre MJ, Palomino-Morales R, Martin M, Delgado JR, et al. The potential role of the glycoprotein osteoactivin/glycoprotein nonmetastatic melanoma protein iB n pancreatic cancer. Pancreas. 2015; 44(2):302–10. https://doi.org/10.1097/MPA.0000000000000250 PMID: 25426614

143. Morandi F, Morandi B, Horenstein AL, Chillemi A, Quarona V, Zaccarello G, et al. A non-canoncial adensinergic pathway led by CD38 in human melanoma cells induces suppression of T cell proliferation. Oncotarget. 2015; 6(28):25602–18. https://doi.org/10.18632/oncotarget.4693 PMID: 26329660

144. Nesmiyanov PP, Tolkachev BE, Strygin AV. ZO-1 expression shows prognostic value in chronic B cell leukemia. Immunobiology. 2016; 221(1):6–11. https://doi.org/10.1016/j.imbio.2015.08.008 PMID: 26306999

145. Zheng D, Liao S, Zhu G, Luo GH, Xiao S, He J, et al. CD38 is a putative functional marker for side population cells in human nasopharyngeal carcinoma cell lines. Mol Carcinog. 2016; 55(3):300–11. https://doi.org/10.1002/mc.22279 PMID: 25630761

146. Poret N, Fu Q, Guihard S, Cheok M, Miller K, Zeng G, et al. CD38 in hairy cell leukemia is a marker of poor prognosis and a new target for therapy. Cancer Res. 2015; 75(18):3902–11. https://doi.org/10.1158/0008-5472.CAN-15-0893 PMID: 26170397

147. Williams KA, Lee M, Hu Y, Andreas J, Patel SJ, Zhang S, et al. A systems genetics approach identifies CXCL14, ITGAX, and LPCAT2 as novel aggressive prostate cancer susceptibility genes. PLoS Genetics. 2014; 10(11):e1004809.

148. Kohsaka S, Hinohara K, Wang L, Nishimura T, Urushido M, Yachi K, et al. Epiregulin enhances tumorigenicity by activing the ERK/MAPK pathway in glioblastoma. Neuro Oncol. 2014; 16(7):960–70. https://doi.org/10.1093/neuonc/not315 PMID: 24470554

149. Riese DJn, Cullum RL. Epiregullin: roles in normal physiology and cancer. Semin Cell Dev Biol. 2014; 28:49–56. https://doi.org/10.1016/j.semcdb.2014.03.005 PMID: 24631357

150. Liu K, Shi Y, Guo XH, Ouyang YB, Wang SS, Liu DJ, et al. Phosphoryalted AKT inhibits the apoptosis induced by DRAM-mediated mitophagy in hepatocellular carcinoma by preventing the translocation of DRAM to mitochondria. Cell Death Dis. 2014; 5:e1078. https://doi.org/10.1038/cddis.2014.51 PMID: 24556693

151. Guan JJ, Zhang XD, Sun W, Qi L, Wu JC, Qin ZH. DRAM1 regulates apoptosis through increasing protein levels and lysosomal localization of BAX. Cell Death Dis. 2015; 6:e1624. https://doi.org/10.1038/cddis.2014.546 PMID: 25633293

152. Cordani M, Butera G, Pacchiana R, Donadelli M. Molecular interplay between mutant p53 proteins and autophagy in cancer cells. Biochim Biophys Acta. 2016; 1867(1):19–28. https://doi.org/10.1016/j.bbcan.2016.11.003 PMID: 27871965

153. Cheng Z, Dai LL, Song YN, Si JM, Xia J, Liu YF. Regulatory effect of iron regulatory protein-2 on iron metabolism in lung cancer. Genet Mol Res. 2014; 13(1):5514–22.

154. Wang W, Deng Z, Hatcher H, Miller LD, Di X, Tesfay L, et al. IRP2 regulates breast tumor growth. Cancer Res. 2014; 74(2):497–507. https://doi.org/10.1158/0008-5472.CAN-13-1224 PMID: 24285726

155. Cheng TC, Tu SH, Chen LC, Chen MY, Chen WY, Lin YK, et al. Down-regulation of alpha-L-fucosidase 1 expression confers inferior survival for triple-negative breast cancer patients by modulating the glycosylation status of the tumor cell surface. Oncotarget. 2015; 6(25):21283–300. https://doi.org/10.18632/oncotarget.4238 PMID: 26204487

156. Mossad NA, Mahmoud EH, Osman EA, Mahmoud SH, Shousha HI. Evluation of squamous cell carcinoma antigen-immunoglobulin M complex (SCCA-IGM) and alpha-L-fucosidase (AFU) as novel diagnostic biomarkerrs for hepaotcellular carcinoma. Tumour Biol. 2014; 35(11):11559–64. https://doi.org/10.1007/s13277-014-2467-y PMID: 25129443

157. Lyu XJ, Li HZ, Ma X, Li XT, Gao Y, Ni D, et al. Elevated S100A6 (Calcyclin) enhances tumorigenesis and suppresses CXCL14-induced apoptosis in clear cell renal cell carcinoma. Oncotarget. 2015; 6(9):6656–69. https://doi.org/10.18632/oncotarget.3169 PMID: 25760073

158. Li Y, Wagner ER, Yan Z, Wang Z, Luther G, Jiang WG, et al. The calcium-binding protein S100A6 accelerates human osteosarcoma growth by promoting cell proliferation and inhibiting osteogenic differentiation. Cell Physiol Biochem. 2015; 37(6):2375–92. https://doi.org/10.1159/000438591 PMID: 26646427

159. Chen X, Liu X, Lang H, Zhang S, Luo Y, Zhang J. S100 calcium-binding protein A6 promotes epithelial-mesenchymal transition through b-catenin in pancreatic cancer cell line. PLoS One. 2015; 10(3):e0121319. https://doi.org/10.1371/journal.pone.0121319 PMID: 25799022

160. Lyu XJ, Li H, Ma X, Li X, Gao Y, Ni D, et al. High-level S100A6 promotes metassis and predicts the outcome of T1-T2 stage in clear cell renal cell carcinoma. Cell Biochem Biophys. 2015; 71(1):279–90. https://doi.org/10.1007/s12013-014-0196-x PMID: 25120023

161. Wang Y, Wang LY, Feng F, Zhao Y, Huang MY, Shao Q, et al. Effect of Raf kinase inhibitor protein expression on malignant biological behavior and progression of colorectal cancer. Oncol Rep. 2015; 34(4):2106–14. https://doi.org/10.3892/or.2015.4157 PMID: 26238523

162. Ping FM, Liu GJ, Liu ZJ, Li HB, Zhai JW, Li SX, et al. Expression of RKIP, E-cadherin and NF-kB in esophageal squamous cell carcinoma and their correlations. Int J Clin Exp Pathol. 2015; 8(9):10164–70. PMID: 26617724

163. Noh HS, Hah YS, Ha JH, Kang MY, Zada S, Rha SY, et al. REgulation of th eepithelial to mesenchymal transition and metastasis by Raf kinase inhibitory protein-dependent Notch1 activity. Oncotarget. 2016; 7(4):4632–46. https://doi.org/10.18632/oncotarget.6728 PMID: 26716415

164. Datar I, Qiu X, Ma HZ, Yeung M, Aras S, de la Serna I, et al. RKIP regullates CCL5 expression to inhibit breast cancer invasion and metastasis by controlling macrophage infiltration. Oncotarget. 2015; 6(36):39050–61. https://doi.org/10.18632/oncotarget.5176 PMID: 26375811

165. Gemoli T, Strohkamp S, Schillo K, Thorns C, Habermann JK. MALDI-imaging reveals thymosin beta-4 as an independent prognostic marker for colorectal cancer. Oncotarget. 2015; 6(41):43869–80. https://doi.org/10.18632/oncotarget.6103 PMID: 26556858

166. Fu X, Cui P, Chen F, Xu J, Gong L, Jiang L, et al. Thymosin beta-4 promotes hepatoblastoma metastasis via induction of epithelial-mesenchymal transition. Mol Med Rpt. 2015; 12(1):127–32.

167. Sharma MC, Tuszynski GP, Blackman MR, Sharma M. Long-term efficacy and downstream mechanism of anti-annexinA2 monoclonal antibody (anti-ANX A2 mAb) in a pre-clinical model of aggressive human breast cancer. Cancer Lett. 2016; 373(1):27–35. https://doi.org/10.1016/j.canlet.2016.01.013 PMID: 26797420

168. Wang T, Yuan J, Zhang J, Tian R, Ji W, Zhou Y, et al. Anxa2 binds to STAT3 and promotes epithelial to mesenchymal transition in breast cancer cells. Oncotarget. 2015; 6(31):30975–92. https://doi.org/10.18632/oncotarget.5199 PMID: 26307676

169. Zhang H, Yao M, Wu W, Qiu L, Sai W, Yang J, et al. Up-regulation of annexin A2 expression predicates advanced clinicopathological features and poor prognosis in hepatocellular carcinoma. Tumour Biol. 2015; 36(12):9373–83. https://doi.org/10.1007/s13277-015-3678-6 PMID: 26109000

170. Gao Q, Zhao YJ, Wang XY, Guo WJ, Gao S, Wei L, et al. Activation mutations in PTPN3 promote cholangeiocarcinoma cell proliferation and migration and are associated with tumor recurrence in patients. Gastroenterology. 2014; 146(5):1397–407. https://doi.org/10.1053/j.gastro.2014.01.062 PMID: 24503127

171. Peters U, Jiao S, Schumacher FR, Hutter CM, Aragaki AKB, J. A., Berndt SI, et al. Identification of Genetic susceptibility loci for colorectal tumors in a genome-wide meta-analysis. Gastroenterology. 2013; 144(4):799–807. https://doi.org/10.1053/j.gastro.2012.12.020 PMID: 23266556

172. Huang J, Gong ZC, Ghosal G, Chen J. SOSS complexes participate in the maintenance of genomic stability. Mol Cell. 2009; 35(3):384–93. https://doi.org/10.1016/j.molcel.2009.06.011 PMID: 19683501

173. Natraian R, Wilkerson PM, Marchio C, Piscuoglio S, Ng CK, Wai P, et al. Characterization of the genomic features and expressed fusion genes in micropapillary carcinomas of the breast. J Pathol. 2014; 232(5):5553–65.

174. Li W, Li K, Zhao L, Zou H. Bioinformatics analysis reveals disturbance mechanism of MAPK signaling pathway and cell cycle in Glioblastoma multiforme. Gene. 2014; 547(2):346–50. https://doi.org/10.1016/j.gene.2014.06.042 PMID: 24967941

175. Diskin SJ, Hou C, Geiessner JT, Attiyeh E.F., Laudenslager M, Bosse K, et al. Copy number variation at 1q21.1 associated with neuroblastoma. Nature. 2009; 459(7249):987–91. https://doi.org/10.1038/nature08035 PMID: 19536264

176. Chen H, Sun B, Zhao Y, Song X, Fan W, Zhou K, et al. Fine mapping of a region of chromosome 11q23.3 reveals independent locus associated with risk of glioma. PLoS One. 2012; 7(12):e52864. https://doi.org/10.1371/journal.pone.0052864 PMID: 23300798

177. Ma Y, Liu L, Yan F, Wei W, Deng J, Sun J. Enhanced expression of long non-coding RNA NEAT1 is associated with the progression of gastric adenocarcinomas. World J Surg Oncol. 2016; 14(1):41. https://doi.org/10.1186/s12957-016-0799-3 PMID: 26911892

178. He C, Jiang B, Ma J, Li Q. Aberrant NEAT1 expression is associated with clinical outcome in high grade glioma patients. APMIS. 2016; 124(3):169–74. https://doi.org/10.1111/apm.12480 PMID: 26582084

179. Wu Y, Yang L, Zhao J, Nie J, Liu F, Zhuo C, et al. Nuclear-enriched abundant transcript 1 as a diagnostic and prognostic biomarker in colorectal cancer. Mol Cancer. 2015; 14:191. https://doi.org/10.1186/s12943-015-0455-5 PMID: 26552600

180. Li Y, Li Y, Chen W, He F, Tan Z, Zheng J, et al. NEAT expression is associated with tumor recurrence and unfavorable prognosis in colorectal cancer. Oncotarget. 2015; 6(29):27641–50. https://doi.org/10.18632/oncotarget.4737 PMID: 26314847

181. Martinez-Iglesias OA, Alonso-Merino E, Gomez-Rey S, Velasco-Martin JP, Martin Orozco R, Luengo E, et al. Autoregulatory loop of nuclear corepressor 1 expression controls invasion, tumor growth, and metastasis. Proc Natl Acad Sci U S A. 2016; 113(3):E328–37. https://doi.org/10.1073/pnas.1520469113 PMID: 26729869

182. van Dijk M, Visser A, Buabeng KM, OPoutsma A, van der Schors RC, Oudejans CB. Mutations with the LINC-HELLP non-coding RNA differentially bind ribosomal and RNA splicing complexes and negatively affect trophoblast differentiation. Hum Mol Genet. 2015; 24(19):5475–85. https://doi.org/10.1093/hmg/ddv274 PMID: 26173455

183. Quidvilloe V, Alsafadi S, Goubar A, Commo F, Scott V, Pioche-Durieu C, et al. Targeting the deregulated splicosome core machinery in cancer cells triggers mTOR blockade and autophagy. Cancer Res. 2013; 73(7):2247–58. https://doi.org/10.1158/0008-5472.CAN-12-2501 PMID: 23358685

184. Shimada K, Ishikawa T, Nakamura F, Shimizu D, Chishima T, Ichikawa Y, et al. Collapsin response mediator protein 2 is involved in regulating breast cancer progression. Breast Cancer. 2014; 21(6):715–23. https://doi.org/10.1007/s12282-013-0447-5 PMID: 23381229

185. Ocak S, Friedman DB, Chen H, Ausborn JA, Hassanein M, Detry B, et al. Discovery of new membrane-associated proteins overexpressed in small-cell lung cancer. J Thorac Oncol. 2014; 9(3):324–36. https://doi.org/10.1097/JTO.0000000000000090 PMID: 24518087

186. Cheng C, Sharp PA. Regulation of CD44 alternative spliciing by SRm160 and its potential role in tumor cell invasion. Mol Cell Biol. 2006; 26(1):362–70. https://doi.org/10.1128/MCB.26.1.362-370.2006 PMID: 16354706

187. Vizeacoumar FJ, Arnold R, Vizeacoumar FS, Chandrashekhar M, Buxzina A, Young JT, et al. A negative genetic interaction map in isogenic cancer cell lines reveals cancer cell vulnerabilities. Mol Syst Biol. 2013; 9:696. https://doi.org/10.1038/msb.2013.54 PMID: 24104479

188. Ni P, Zhang Y, Liu Y, Lin X, Su X, Lu H, et al. HMGB1 silence could promote MCF-7 cell apoptosis. Int J Clin Exp Pathol. 2015; 8(12):15940–6. PMID: 26884867

189. Beheshti Zavareh R, Sukhai MA, Hurren R, Goronda M, Wang X, Simpson CD, et al. Suppression of cancer progression by MGAT1 shRNA knockdown. PLoS One. 2012; 7(9):e43721. https://doi.org/10.1371/journal.pone.0043721 PMID: 22957033

190. Ni P, Zhang Y, Liu Y, Lin X, Su X, Lu H, et al. HMGB1 silence could promote MCF-7 cell apoptosis andinhbit invasion and metastasis. Int J Clin Exp Pathol. 2015; 8(12):15940–6. PMID: 26884867

191. Chen YC, Statt S, Wu R, Chang HT, Liao JW, WAng CN, et al. High mobility group box 1-induced epithelial mesenchymal transition in human airway epithelial cells. Sci Rep. 2016; 6:18815. https://doi.org/10.1038/srep18815 PMID: 26739898

192. Shrivastava S, Mansure JJ, Almajed W, Cury F, Ferbeyre G, Popovic M, et al. The role of HMGB1 in radioresistance of bladder cancer. Mol Cancer Ther. 2016; 15(3):471–9. https://doi.org/10.1158/1535-7163.MCT-15-0581 PMID: 26719575

193. Marques E, Englund JI, Tervonen TA, Virkunen E, Laakso M, Myllynen M, et al. Par6G suppresses cell proliferation and is targeted by loss-of-function mutations inmultiple cancers. Oncogene. 2016; 35(11):1386–98. https://doi.org/10.1038/onc.2015.196 PMID: 26073086

194. Whitworth H, Bhadel S, Ivey M, Conaway M, Spencer A, Hernan R, et al. Identification of kinase regulating prostate cancer celll growth using an RNAi phenotypic screen. PLoS One. 2012; 7(6):e38950. https://doi.org/10.1371/journal.pone.0038950 PMID: 22761715

195. Yang Y, Roine N, Makela TP. CCRK depletion inhibits glioblastoma cell proliferation in a cilium-dependent manner. EMBO Rep. 2013; 14(8):741–7. https://doi.org/10.1038/embor.2013.80 PMID: 23743448

196. Makkonen H, Jaaskelainen T, Pitkanen-Arsiola T, Rytinki M, Waltering KK, Matto M, et al. Identification fo ETS-like transcription factor 4 as a novel androgen receptor target in prostate cancer. Oncogene. 2008; 27(36):4865–76. https://doi.org/10.1038/onc.2008.125 PMID: 18469865

197. Peng C, Zeng W, Su JJ, Kuang Y, He Y, Zhao S, et al. Cyclin-dependent kinase 2 (CDK2) is a key mediator for EGF-induced cell transformation mediated through the ELK4/c-Fos signaling pathway. Oncogene. 2016; 35(9):1170–9. https://doi.org/10.1038/onc.2015.175 PMID: 26028036

198. Irandoust M, Alvarez Zarate J, Hubeek I, van Beek EM, Schornagel K, Broekhuizen AJ, et al. Engagement of SIRPalpha inhibits growth and induces programmed cell death in acute myeloid leukemia cells. PLoS One. 2013; 8(1):e52143. https://doi.org/10.1371/journal.pone.0052143 PMID: 23320069

199. Theocharides AP, Jin L, Cheng PY, Prasolava TK, Malko AV, Ho JM, et al. Disruption of SIRPalpha signaling macrophages eliminates human acute myeloid leukemia stem cells in xenografts. J Exp Med. 2012; 209(10):1883–99. https://doi.org/10.1084/jem.20120502 PMID: 22945919

200. Cheong JY, Kim YB, Woo JH, Kim DK, Yeo M, Yang SJ, et al. Identification of NUCKS1 as a putative oncogene and immunodiagnostic marker of hepatocellular carcinoma. Gene. 2016; 584(1):47–53. https://doi.org/10.1016/j.gene.2016.03.006 PMID: 26968889

201. Gu LH, Xia B, Zhong L, Ma Y, Liu L, Yang L, et al. NUCKS1 overexpression is a novel biomarker for recurrence-free survival in cervical squamous cell carcinoma. Tumour Biol. 2014; 35(8):7831–6. https://doi.org/10.1007/s13277-014-2035-5 PMID: 24819170

202. Kikuchi M A., Ishikawa T, Mogushi K, Ishiguro M, Iida S, et al. Identification of NUCKS1 as a colorectal cancer prognostic marker through integrated expression and copy number analysis. Int J Cancer. 2013; 132(10):2295–302. https://doi.org/10.1002/ijc.27911 PMID: 23065711

203. Namiki T, Coelho SG, Hearing VJ. NAUK2: an emerging acral melanoma oncogene. Oncotarget. 2011; 2(9):695–704. https://doi.org/10.18632/oncotarget.325 PMID: 21911917

204. Namiki T, Tanemura A, Valencia JC, Coelho SG, Passeron T, Kawaguchi M, et al. AMP kinase-related kinase NUAK2 affects tumor growth, migration, and clinical outcome of human melanoma. Proc Natl Acad Sci U S A. 2011; 108(16):6597–602. https://doi.org/10.1073/pnas.1007694108 PMID: 21460252

205. Yamaguchi H, Ding Y, Lee JF, Zhang M, Pal A, Bornmann W, et al. Interferon-inducible protein IFIXa inhibits cell invasion by upregulating the metastasis suppressor maspin. Mol Carcinog. 2008; 47 (10):739–43. https://doi.org/10.1002/mc.20423 PMID: 18247378

206. Damaghi M, Tafreshi NK, Lloyd MC, Sprung R, Estrella V, Woitkowiak JW, et al. Chronic acidosis in the tumour microenvironment selects for overexpression of LAMP2 in the plasma membrane. Nat Commun. 2015; 6:8752. https://doi.org/10.1038/ncomms9752 PMID: 26658462

207. Huang CF, Deng WW, Zhang L, Zhang WF, Sun ZJ. Expression of LC3, LAMP2, KEAP1 and NRF2 in salivary adenoid cystic carcinoma. Pathol Oncol Res. 2016; 22(1):109–14. https://doi.org/10.1007/s12253-015-9981-0 PMID: 26350055

208. Jiang JL, Chen X, She J, Wei Y, Wu T, Yang Y, et al. Beta1,4-galactosyltransferase V functions as a positive growth regulator in glioma. J Biol Chem. 2006; 281(14):9482–9. https://doi.org/10.1074/jbc.M504489200 PMID: 16461357

209. Zhou H, Ma H, Wei W, Ji D, Song X, Sun J, et al. B4GALT family mediates the multidrug resistance of human leukemia cells by regulating the hedgehog pathway and the expression of p-glycoprotein and multidrug- resistance-associated protein 1. Cell Death Dis. 2013; 4:e654. https://doi.org/10.1038/cddis.2013.186 PMID: 23744354

210. Sato T, Furukawa K. Sequential action of Ets-1 and Sp1 in the activation of the human beta-1,4-galactosyltransferase V gene involved in abnormal glycosylation characteristic of cancer cells. J Biol Chem. 2007; 282(38):27702–12. https://doi.org/10.1074/jbc.M611862200 PMID: 17656364

211. Sun YL, Cai JQ, Liu F, Bi XY, Zhou LP, Zhao XH. Aberrant expression of peroxiredoxin 1 and its clinical implications in liver cancer. World J Gastroenterol. 2015; 21(38):10840–52. https://doi.org/10.3748/wjg.v21.i38.10840 PMID: 26478675

212. Bankovic J, Stojsic J, Jovanovic D, Andjelkovic T, Milinkovic V, Ruzdijic S, et al. Identification of genes associated wiht non-small-cell lung cancer promotion and progression. Lung Cancer. 2010; 67 (2):151–9. https://doi.org/10.1016/j.lungcan.2009.04.010 PMID: 19473719

213. Hua M, Yan S, Deng Y, Xi Q, Liu R, Yang S, et al. CAP1 is overexpressed in human epithelial ovarian cancer and promotes cell proliferation. Int J Mol Med. 2015; 35(4):941–9. https://doi.org/10.3892/ijmm.2015.2089 PMID: 25652936

214. Xie SS, Tan M, Lin HY, Xu L, Shen CX, Yuan Q, et al. Overexpression of adenylate cyclase = associated protein 1 may predict brain metastasis in non-small cell lung cancer. Oncol Rep. 2015; 33 (1):363–71. https://doi.org/10.3892/or.2014.3577 PMID: 25371324

215. Yu XF, Ni QC, Chen JP, Xu JF, Jiang Y, Yang SY, et al. Knocking down th eexpression of adenylate cyclase-associated protein 1 inhibits the proliferation and migration of breast cancer cells. Exp Mol Pathol. 2014; 96(2):188–94. https://doi.org/10.1016/j.yexmp.2014.02.002 PMID: 24509166

216. Liu Y, Cui X, Hu B, Huang X, Cai JQ, He S, et al. Upregulated expression of CAP1 is associated with tumor igration and metastsis in hepatocellular carcinoma. Pathol Res Pract. 2014; 210(3):169–75. https://doi.org/10.1016/j.prp.2013.11.011 PMID: 24359721

217. Zhang J, Guo H, Qian G, Ge S, Ji H, Hu X, et al. MiR-145, a new regulator of the DNA fragmentation factor-45 (DFF45)-mediated apoptotic network. Mol Cancer. 2010; 9:211. https://doi.org/10.1186/1476-4598-9-211 PMID: 20687965

218. Leber B, Maier B, Fuchs F, Chi J, Riffel P, Anderhub S, et al. Proteins required for centrosome clustering in cancer cells. Sci Transl Med. 2010; 2(33):33ra8.

219. Kosaka Y, Mimori K, Tanaka F, Inoue H, Watanabe M, Mori M. Clinical significance of the loss of MATS1 mRNA expression in colorectal cancer. Int J Oncol. 2007; 31(2):333–8. PMID: 17611689

220. Bai J, Adriani G, Dang TM, Tu TY, Penny HX, Wong SC, et al. Contact-dependent carcinoma aggregate dispersion by M2a macrophages via ICAM1 and b-integrin interactions. Oncotarget. 2015; 6 (28):25295–307. https://doi.org/10.18632/oncotarget.4716 PMID: 26231039

221. Eun YG, Kim SK, Chung JH, Kwon KH. Association study of integrins beta 1 and beta 2 gene polymorphism and papillary thyroid cancer. Am J Surg. 2013; 205(6):631–5. https://doi.org/10.1016/j.amjsurg.2012.05.035 PMID: 23388428

222. Chong YK, Sandanaraj E, Koh LW, Thangaveloo M, Tan MS, Koh GR, et al. ST3GAL1-associated transcriptomic progam in glioblastoma tumor growth, invasion, and prognosis. J Natl Cancer Inst. 2015; 108(2):pii: djv326.

223. Picco G, Julien S, Brockhausen I, Beatson R, Antonopoulos A, Haslam S, et al. Over-expression of ST3Gal-1 promotes mammary tumorigenesis. Glycobiology. 2010; 20(10):1241–50. https://doi.org/10.1093/glycob/cwq085 PMID: 20534593

224. Videira PA, Correia M, Malagolini N, Crespo HJ, Ligeiro D, Calais FM, et al. ST3Ga;.1 sialyltransferase relevance in bladder cancer tissues and cell lines. BMC Cancer. 2009; 9:357. https://doi.org/10.1186/1471-2407-9-357 PMID: 19811634

225. Borin TF, Arbab AS, Gelaleti GB, Ferreira LC, Moschetta MG, HJardim-Perassi BV, et al. Melatonin decreases breast cancer metastasis by modulating Rho-associated kinase protein-1. J Pineal Res. 2016; 60(1):3–15. https://doi.org/10.1111/jpi.12270 PMID: 26292662

226. Xue H, Guo X, Han X, Yan S, Zhang J, Xu S, et al. MicroRNA = 584-3p, a novel tumor suppressor and prognostic marker, reduces the migration and invasion of human glioma cells by targeting hypoxia-induced ROCK1. Oncotarget. 2016; 7(4):4785–805. https://doi.org/10.18632/oncotarget.6735 PMID: 26715733

227. Wermke M, Camgoz A, Paszkowski-Rogacz M, Thieme S, von Bonin M, Dahl A, et al. RNAi profiling of primary human AML cells identifies RCOK1 as a therapeutic target and nominates fasudil as an antileukemic drug. Blood. 2015; 125(24):3760–8. https://doi.org/10.1182/blood-2014-07-590646 PMID: 25931586

228. Lin CH, Chung MY, Chen WB, Chien CH. Growth inhibitory effect of the human NIT2 genes and its allelic imbalance in cancers. FEBS J. 2007; 274(11):2946–56. https://doi.org/10.1111/j.1742-4658.2007.05828.x PMID: 17488281

229. Jeong SM, Hwang S, Seong RH. Transferrin receptor regulates pancreatic cancer growth by modulating mitochondrial respiration and ROS generation. Biochem Biophys Res Commun. 2016; 471 (3):373–9. https://doi.org/10.1016/j.bbrc.2016.02.023 PMID: 26869514

230. Zhang M, Cui F, Lu S, JIang T, Chen J, Zhang X, et al. Increased expression of prothymosin-a, independently or combined with TP53, correlates with poor prognosis in colorectal cancer. Int J Clin Exp Pathol. 2014; 7(8):487–76.

231. Glaser J, Neumann MH, Mei Q, Betz BL, Seier N, BEyer I, et al. Macrophage capping protein CapG is a putative oncogene involved in migration and invasiveness in ovarian carcinoma. Biomed Res Int. 2014; 2014:379847. https://doi.org/10.1155/2014/379847 PMID: 24804218

232. Ichikawa H, Kanda T, Kosugi S, Kawachi Y, Sasaki H, Wakai T, et al. Laser microdissection and two-dimensional difference gel electrophoresis reveals the role of a novel macrophage-capping protein in lymph node metastasis in gastric cancer. J Proteome Res. 2013; 12(8):3780–91. https://doi.org/10.1021/pr400439m PMID: 23782053

233. Wang X, Liu H, Zhao C, Li W, Chen Y. THE DEAD-box RNA helicase 51 controls non-small cell lung cancer proliferation by regulating cell cycle progression via multiple pathways. Sci Rep. 2016; 6:26108. https://doi.org/10.1038/srep26108 PMID: 27198888

234. Kindrat I, Tryndyak V, De Conti A, Shpyleva S, Mudalige TK, Kobets T, et al. MicroRNA-152-mediated dysregulation of hepatic transferrin receptor 1 in liver carcinogenesis. Oncotarget. 2016; 7(2):1276–87. https://doi.org/10.18632/oncotarget.6004 PMID: 26657500

235. Yang L, Tao T, Wang Y, Bao Z, He X, Cui G. Knocking down the expression of TRA2beta inhibits the proliferation and migration of human glioma cells. Pathol Res Pract. 2015; 211(10):731–9. https://doi.org/10.1016/j.prp.2015.04.014 PMID: 26298634

236. Diao Y, Wu DC, Dai Z, Kang HJ, Wang Z, Wang X. Prognostic value of transformer 2beta expression in prostate cancer. Int J Clin Exp Pathol. 2015; 8(6):6967–73. PMID: 26261585

237. Ji L, Ni T, Shen Y, Xue Q, Liu Y, Chen B, et al. Transformer 2beta (Tra2b/SFRS10) positively regulates the progression of NSCLC via promoting cell proliferation. J Mol Histol. 2014; 45(5):573–82. https://doi.org/10.1007/s10735-014-9582-3 PMID: 24952301

238. Xiaobo Y, Qiang L, Xiong Q, Zheng R, Jianhua Z, Zhifeng L, et al. Serum and glucocorticoid kinase 1 promoted the growth and migration of non-small cell lung cancer cells. Gene. 2016; 576(1Pt2):339–46.

239. Woo T, Okudela K, Mitsui H, Tajiri M, Rino Y, Ohashi K, et al. Up-regulation of S100A11 in lung adenocarcinoma—Its potential relationship with cancer progression. PLoS One. 2015; 10(11):e142642.

240. Anania MC, Miranda C, Vizioli MG, Mazzoni M, Cleris L, Pagliardini S, et al. SW100A11 overexpression contributes to the malignant phenotype of papillary thyroid carcinoma. J Clin Endocrinol Metab. 2013; 98(10):E1591–600. https://doi.org/10.1210/jc.2013-1652 PMID: 23928665

241. Shindo-Okada N, Iigo M. Expression of the Arp11 gene suppresses the tumorigenicity of PC-14 human lung adenocarcinoma cells. Biochem Biophys Res Commun. 2003; 312(4):889–96,. PMID: 14651955

242. Chen MB, Li C, Shen WX, Guo YJ, Shen W, Lu PH. Association of a LSP1 gene rs3817189>C polymiorphism with breast cancer risk: evidence from 33,920 cases and 35,671 controls. Mol Biol Rep. 2011; 38(7):4687–95. https://doi.org/10.1007/s11033-010-0603-3 PMID: 21127985

243. Chen H, Qi X, Qiu P, Zhao J. Correlation between LSP1 polymorphisms and the susceptibility to breast cancer. Int J Clin Exp Pathol. 2015; 8(5):5798–802. PMID: 26191300

244. Park SL, Fesinmeyer MD, Timofeeva M, Caberto CP, Kocarnik JM, Han Y, et al. Pleiotropic associations of risk variants identified for other cancers with lung cancer risk: the PAGE and TRICL consrotia. J Natl Cancer Inst. 2014; 106(4):dju061. https://doi.org/10.1093/jnci/dju061 PMID: 24681604

245. Zeng WL, Chen YW, Zhou H, Zhou JY, Wei M, Shi R. Expression of HERC4 in lung cancer and its correlation with clincopathological parameters. Asian Pac J Cancer Prev. 2015; 16(2):513–7. PMID: 25684480

246. Wang SJ, Cui HY, Liu YM, Zhao P, Zhang Y, Fu ZG, et al. CD147 promotes Src-dependent activation of Rac1 signaling through STAT3/DOCK8 during the motility of hepatocellular carcinoma cells. Oncotarget. 2015; 6(1):243–57. https://doi.org/10.18632/oncotarget.2801 PMID: 25428919

247. Takahashi K, Kohno T, Ajima R, Saaki H, Minna JD, Fujiwara T, et al. Homozygous deletion and reduced expression of the DOCK8 gene in human lung cancer. Int J Oncol. 2006; 28(2):321–8. PMID: 16391785

248. Mansfield J, Collin P, Collins MO, Choudhary JS, Pines J. APC15 drives the turnover of MCC-CDC20 to make the spindle assembly checkpoint responsive to kinetochore attachment. Nat Cell Biol. 2011; 13(10):1234–43. https://doi.org/10.1038/ncb2347 PMID: 21926987

249. Gong ZY, Kidova H, Mohri T, Han Y, Takakura N. DNA damage enhanced by the attenuation of SLD5 delays cell cycle restoration in normal cells but not in cancer cells. PLoS One. 2014; 9(10):e110483. https://doi.org/10.1371/journal.pone.0110483 PMID: 25334017

250. Barkley LR, Song IY, Zou Y, Vaziri C. Reduced expression of GINS complex members induces hallmarks of pre-malignancy in primary untransformed human cells. Cell Cycle. 2009; 8(10):1577–88. https://doi.org/10.4161/cc.8.10.8535 PMID: 19377277

251. Nikkuni O, Kaira K, Toyoda M, Shino M, Sakakura K, Takahashi K, et al. Expression of amino acid transporters (LAT1 and ASCT2) in patients with Stage III/IV laryngeal squamous cell carcinoma. Pathol Oncol Res. 2015; 21(4):1175–81. https://doi.org/10.1007/s12253-015-9954-3 PMID: 26024742

252. Wang Q, Hardie RA, Hoy AJ, van Geldermalsen M, Gao D, Fazli L, et al. Targeting ASCT2-mediated glutamine uptake blocks prostate cancer growth andtumour development. J Pathol. 2015; 236 (3):278–89. https://doi.org/10.1002/path.4518 PMID: 25693838

253. Karlsson E, Veenstra C, Emin S, Dutta C, Perez-Tenorio G, Nordenskjold B, et al. Loss of protein tyrosine phosphatase, non-receptor type 2 is associated with activation of AKT and tamoxifen resistance in breast cancer. Breast Can Res Treat. 2015; 153(1):31–40.

254. Scharl M, Rogler G. The role for protein tyrosine nonreceptor type 2 in regulating autophagosome formation. Ann N Y Acad Sci. 2012; 1257:93–102. https://doi.org/10.1111/j.1749-6632.2012.06578.x PMID: 22671594

255. Rutkowski MJ, Sughrue ME, Kane AJ, Kim JM, Bloch O, Parsa AT. Epidermal growth factor module-containing mucin-like receptor 2 is a newly identified adhesion G protein-coupled receptor associated with poor overall survival and an invasive phenotype in glioblastoma. J Neurooncol. 2011; 105 (2):165–71. https://doi.org/10.1007/s11060-011-0576-7 PMID: 21503828

256. Davies JQ, Lin HH, Stacey M, Yona S, Chang GW, Gordon S, et al. Leukocyte adhesion-GPCR EMR2 is aberrantly expressed in human breast carcinomas and is associated with patient survival. Oncol Rep. 2011; 25(3):619–27. https://doi.org/10.3892/or.2010.1117 PMID: 21174063

257. Patani N, Jiang WG, Mokbel K. Prognostic utility of glycosyltransferase expression in breast cancer. Cancer Genomics Proteomics. 2008; 5(6):333–40. PMID: 19287074

258. Gomes J, Marcos NT, Berois N, Osinaga E, Magalhaes A, Pinto-de-Sousa J, et al. Expression of UDP-N-acetyl-D-galactosamine: polypeptide N-acetylgalactosaminyltransferase-6 in gastric mucosa, intestinal metaplasia, and gastric carcinoma. J Histochem Cytochem. 2009; 57(1):79–86. https://doi.org/10.1369/jhc.2008.952283 PMID: 18854599

259. Chen CH, Cheng CT, Yuan Y, Zhai J, Arif M, Fong LW, et al. Elevated MARCKS phosphorylation contributes to unresponsiveness of breast cancer to paclitaaxel treatment. Oncotarget. 2015; 6 (17):15194–208. https://doi.org/10.18632/oncotarget.3827 PMID: 26015406

260. Chen C, H, Statt S, Chiu CL, Thai P, Arif M, Adler KB, et al. Targeting myristolated alanine-rich C kinase substrate phosphorylation site domain in lung cancer. Mechanisms and therapeutic implication. Am J Respir Crit Care Med. 2014; 190(10):1127–38. https://doi.org/10.1164/rccm.201408-1505OC PMID: 25318062

261. Bickeboller M, Tagscherer KE, Kloor M, Jansen L, Chang-Claude J, Brenner H, et al. Functional characterization of the tumor-suppressor MARCKS in colorectal cancer and its association with survival. Oncogene. 2015; 34(9):1150–9. https://doi.org/10.1038/onc.2014.40 PMID: 24662837

262. Yang Y, Chen Y, Saha MN, Chen J, Evans KW, Qiu L, et al. Targeting phospho-MARCKS overcomes drug-resistance and induces antitumor activity in preclinical models of multiple myeloma. Leukemia. 2015; 29(3):715–26. https://doi.org/10.1038/leu.2014.255 PMID: 25179733

263. Rohrbach TD, Jarboe JS, Anderson JC, Trummell HQ, Hicks PH, Weaver AN, et al. Targeting the effector domain of the myristolated alanine rich C-kinase substrate enhances lung cancer radiation sensitivity. Int J Oncol. 2015; 46(3):1079–88. https://doi.org/10.3892/ijo.2014.2799 PMID: 25524703

264. Tan CP, Qiao F, Wei P, Chi Y, Wang W, Ni S, et al. DIXC1 activates Wnt signaling pathway and promotes gastric cancer cell invasion and metastasis. Mol Carcinog. 2016; 55(4):397–408. https://doi.org/10.1002/mc.22290 PMID: 25648220

265. Gao X, Mi Y, Yan AC, Sha B, Guo N, Hu Z, et al. The PHLDB1 re498872 (11q23.3) polymorphism and glioma risk: A meta-analysis. Asian Pac J Cancer Prev. 2015; 11(4):e13–21.

266. Baskin R, Woods NT, Mendoza-Fandino G, Forsyth P, Egan KM, Monteiro AN. Functional analysis of the 11q23.3 glioma susceptibility locus implicaates PHLDB1 and DDX6 in glioma susceptibility. Sci Rep. 2015; 5:17367. https://doi.org/10.1038/srep17367 PMID: 26610392

267. Solimini NL, Liang AC, Xu C, Pavlova NN, Xu Q, Davoli T, et al. STOP gene Phactr4 is a tumor suppressor. Proc Natl Acad Sci U S A. 2013; 110(5):E407–14. https://doi.org/10.1073/pnas.1221385110 PMID: 23319639

268. Cheng JC, Bai A, Beckham TH, Marrison ST, Yount CL, Lu PY, et al. Radiation-induced acid ceramidase confers prostate cancer resistance and tumor relapse. J Clin Invest. 2013; 123(10):4344–58. https://doi.org/10.1172/JCI64791 PMID: 24091326

269. Roh JL, Park JY, Kim EH, Jang HJ. Targeting acid ceramidase sensitises head and neck cancer to cisplatin. Eur J Cancer. 2016; 52:163–72. https://doi.org/10.1016/j.ejca.2015.10.056 PMID: 26687835

270. Realini N, Palese F, Pizzirani D, Pontis S, Basit A, Bach A, et al. Acid ceramidase in melanoma: expression, localization, and effrects of pharmacological inhibition. J Biol Chem. 2016; 291(5):2422–34. https://doi.org/10.1074/jbc.M115.666909 PMID: 26553872

271. Li R, Liu GZ, Luo SY, Chen R, Zhang JX. Cyclin I promotes cisplatin resistance via Cdk5 activation in cervical cancer. Eur Rev Med Pharmacol Sci. 2015; 19(23):4533–41. PMID: 26698249

272. Sun ZL, Zhu Y, Wang FQ, Chen R, Peng T, Fan ZN, et al. Serum proteomic-based analysis of pancreatic carcinoma for the identification of potential cancer biomarkers. Biochim Biophys Acta. 2007; 1774 (6):764–71. https://doi.org/10.1016/j.bbapap.2007.04.001 PMID: 17507299

273. Thai P, Statt S, Chen CH, Liang E, Campbell C, Wu R. Characterization of a novel long noncoding RNA, SCAL1, induced by cigarette smoke and elevated in lung cancer cell lines. Am J Respir Cell Mol Biol. 2013; 49(2):204–11. https://doi.org/10.1165/rcmb.2013-0159RC PMID: 23672216

274. Renhua G, Yue S, Shidai J, JIng F, Ziyi L. 165P: Long noncoding RNA LUCAT1 is associated with poor prognosis in human non-small cell lung cancer and affects cell proliferation via regulating p21 and p57 expression. J Thorac Oncol. 2016; 11(4 Supp):S129.

275. Zheng ZG, NXu H, Suo SS, Xu XL, Ni MW, Gu LH, et al. The essential role of H19 contributing to cisplatin resistance by regulating glutathioine metabolism in high-grade serous ovarian cancer. Sci Rep. 2016; 6:26093. https://doi.org/10.1038/srep26093 PMID: 27193186

276. Ali-Rahmani F, Fitzgerald DJ, Martin S, Patel P, Prunotto M, Ormanoglu P, et al. Anticancer effects of mesothelin-targeted immunotoxin theapy are regulated by tyrosine kinase DDR1. Cancer Res. 2016; 76(6):1560–8. https://doi.org/10.1158/0008-5472.CAN-15-2401 PMID: 26719540

277. Huo Y, Yang M, Lie W, WYang J, Fu XT, Liu DJ, et al. High expression of DDR1 is associated with the poor prognosis in Chinese patients with pancreatic ductal adenocarcinoma. J Exp Clin Cancer Res. 2015; 34:88. https://doi.org/10.1186/s13046-015-0202-1 PMID: 26297342

278. De Smaele E, Di Marcotullio L, Moretti M, Pelloni M, Occhione MA, Infante P, et al. Identification and characterization of KCASH2 and KCASH3, 2 novel Cullin3 adaptors suppressing histone deacetylase and Hedgehog activity inmedulloblastoma. Neoplasia. 2011; 13(4):374–85. PMID: 21472142